

Nickel Thioether Chemistry: Synthesis, Structures and Electrochemistry of Five-co-ordinate Nickel(II) Complexes of [9]aneS₃. Crystal Structures of [Ni([9]aneS₃)- (dppm)][PF₆]₂, [Ni([9]aneS₃)(dcpe)][PF₆]₂·1.25MeCN and [Ni([9]aneS₃)(tdpme)][PF₆]₂ {[9]aneS₃ = 1,4,7-Trithia- cyclononane, dppm = Ph₂PCH₂PPh₂, dcpe = (C₆H₁₁)₂- PC₂H₄P(C₆H₁₁)₂, tdpme = CH₃C(CH₂PPh₂)₃}†

Alexander J. Blake, Robert O. Gould, Malcolm A. Halcrow and Martin Schröder *

Department of Chemistry, The University of Edinburgh, West Mains Road, Edinburgh EH9 3JJ, UK

Reaction of [Ni(L-L)Cl₂] {L-L = Ph₂PCH₂PPh₂ (dppm), R₂PCH₂CH₂PR₂ [R = Ph (dppe), C₆H₁₁ (dcpe) or Me (dmpe)], *cis*-Ph₂PCH=CHPPh₂ (dppv), Ph₂PCH₂CH₂CH₂PPh₂ (dppp) or MeC(CH₂PPh₂)₃ (tdpme)} with 1 molar equivalent of 1,4,7-trithiacyclononane([9]aneS₃) afforded the complex cations [Ni([9]aneS₃)(L-L)]²⁺. The crystal structures of [Ni([9]aneS₃)(dppm)][PF₆]₂, [Ni([9]aneS₃)(dcpe)][PF₆]₂·1.25MeCN and [Ni([9]aneS₃)(tdpme)][PF₆]₂ showed five-co-ordinate complexes with distorted square-pyramidal geometries about the nickel(II) centres with the S-donors of [9]aneS₃ occupying two basal and the apical position, Ni-S_{apical} 2.40–2.65 Å, Ni-S_{basal} 2.22–2.27 Å, Ni-P_{basal} 2.17–2.22 Å. The complex [Ni([9]aneS₃)(dppm)][PF₆]₂ crystallises in triclinic space group $\bar{P}\bar{1}$, $a = 10.9748(25)$, $b = 13.9702(20)$, $c = 15.7688(24)$ Å, $\alpha = 80.071(7)$, $\beta = 70.817(8)$, $\gamma = 76.441(8)$ °, $D_c = 1.374$ g cm⁻³, $Z = 2$; [Ni([9]aneS₃)(dcpe)][PF₆]₂·1.25MeCN crystallises in triclinic space group $\bar{P}\bar{1}$, $a = 12.432(8)$, $b = 13.382(4)$, $c = 15.070(6)$ Å, $\alpha = 86.83(2)$, $\beta = 70.47(2)$, $\gamma = 77.28(2)$ °, $D_c = 1.445$ g cm⁻³, $Z = 2$; [Ni([9]aneS₃)(tdpme)][PF₆]₂ crystallises in monoclinic space group Cc , $a = 10.7597(16)$, $b = 37.399(5)$, $c = 13.104(3)$ Å, $\beta = 103.746(11)$ °, $D_c = 1.491$ g cm⁻³, $Z = 4$. Cyclic voltammetry of the complexes [Ni([9]aneS₃)(L-L)][PF₆]₂ in MeCN (0.1 mol dm⁻³ NBu₄PF₆) at 293 K at platinum electrodes showed one chemically reversible and one quasi-reversible one-electron reduction at $E_{1/2} = -0.77$ to -1.16 V, $\Delta E_p = 61$ – 92 mV, $E_{3/2} = -1.31$ to -1.93 V vs. ferrocene–ferrocenium. On the basis of ESR and electronic spectroscopy, these reduction products are assigned as pyramidal d⁹ nickel(I) [Ni([9]aneS₃)(L-L)]⁺ with binding of both P-donors retained, and tetrahedral d¹⁰ nickel(0) [Ni([9]aneS₃)(L-L)]⁰ species respectively. The reaction of [Ni([9]aneS₃)(L-L)]⁺ with CO in MeCN is discussed.

The chemistry of nickel in the +1 and +3 oxidation states has attracted intense interest.¹ This is due to both the discovery of redox-active nickel sites in methyl co-enzyme A reductase (Factor 430), CO oxido-reductase and several hydrogenase enzymes,² and the known ability of nickel(I) complexes to bind and activate substrates such as CO,³ CO₂,⁴ SO₂,⁵ and alkyl halides.^{6,7} As part of our structural and electrochemical studies of polythia macrocyclic complexes,⁸ we have shown that oxidation of the homoleptic hexathia species [Ni([9]aneS₃)₂]²⁺ ([9]aneS₃ = 1,4,7-trithiacyclononane) leads to the formation of a relatively stable octahedral d⁷ nickel(III) species [Ni([9]aneS₃)₂]³⁺.⁹ Reduction of [Ni([9]aneS₃)₂]²⁺ however gives a highly unstable nickel(I) species which readily decomposes in solution.^{9,10} We argued that the instability of [Ni([9]aneS₃)₂]⁺ was partly stereochemical in origin, since the [9]aneS₃ ligand set is known to afford unusually stable mononuclear d⁹ complexes [M([9]aneS₃)₂]²⁺ (M = Ag¹¹ or Au^{12,13}). We felt that a five co-ordinate donor set including the [9]aneS₃ ligand might stabilise nickel(I) more effectively.

We report herein the synthesis, structures and electro-

chemistry of a series of complex cations [Ni([9]aneS₃)-(L-L)]²⁺ (L-L = diphosphine chelate).

Results and Discussion

Reaction of [Ni(L-L)Cl₂] {L-L = bis(diphenylphosphino)methane (dppm), 1,2-bis(diphenylphosphino)ethane (dppe), *cis*-1,2-bis(diphenylphosphino)ethene (dppv), 1,2-bis(dicyclohexylphosphino)ethane (dcpe), 1,2-bis(dimethylphosphino)ethane (dmpe), 1,3-bis(diphenylphosphino)propane (dppp) or 1,1,1-tris(diphenylphosphinomethyl)ethane (tdpme)}¹⁴ with 1 molar equivalent of [9]aneS₃ in either refluxing MeOH followed by anion metathesis with NH₄PF₆, or in MeNO₂ at 293 K in the presence of 2 molar equivalents of TiPF₆, affords the dark green (L-L = dppm, dppe, dppv, dppp or tdpme) or red (L-L = dcpe or dmpe) crystalline compounds [Ni([9]aneS₃)(L-L)][PF₆]₂. Fractional recrystallisation from MeCN–Et₂O is necessary to remove the pink by-product [Ni([9]aneS₃)₂][PF₆]₂; this contamination is particularly severe for complexes containing strained or sterically crowded diphosphine ligands (L-L = dppm, dcpe or dppp). Preliminary attempts to synthesise analogous complexes [Ni([9]aneS₃)(PR₃)₂]²⁺ (R = Ph or Et) and [Ni([9]aneS₃)(L-L)]²⁺ (L-L = 2,2'-bipyridine (bipy), 1,10-phenanthroline (phen) or Ph₂AsCH₂CH₂AsPh₂) by similar methods afforded [Ni([9]aneS₃)₂]²⁺ as the only

† Supplementary data available: see Instructions for Authors, *J. Chem. Soc., Dalton Trans.*, 1993, Issue 1, pp. xxiii–xxviii.

Non-SI unit employed: G = 10⁻⁴ T.

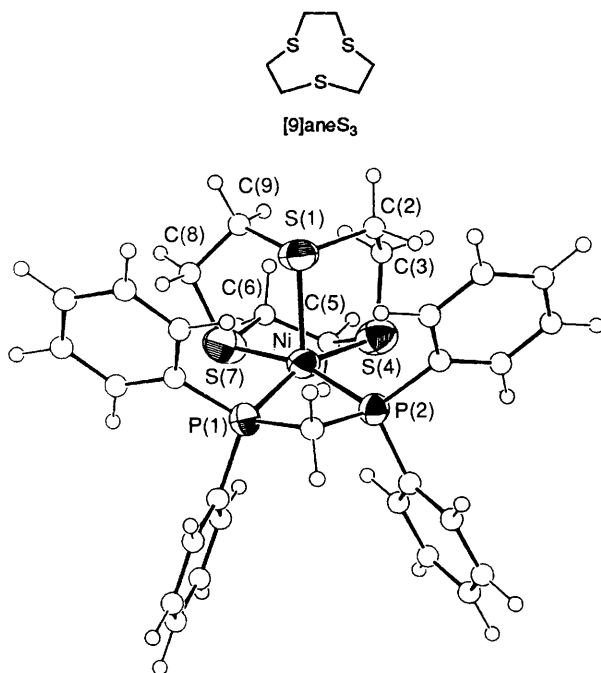


Fig. 1 Single-crystal structure of $[\text{Ni}([\text{9}]\text{aneS}_3)(\text{dppm})]^{2+}$ with numbering scheme adopted

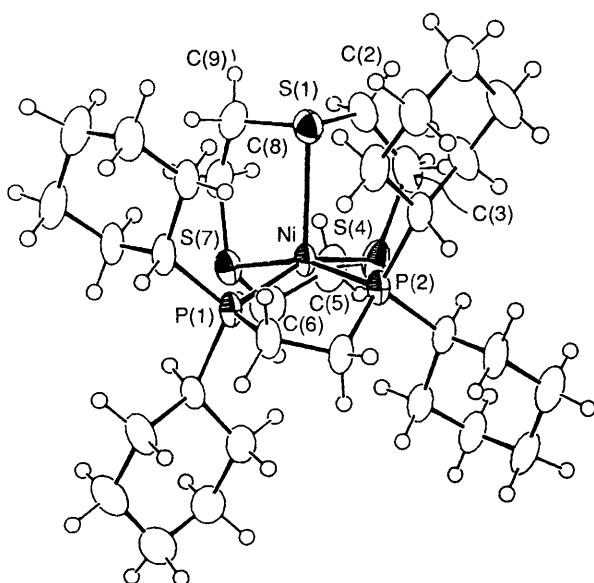


Fig. 2 Single-crystal structure of $[\text{Ni}([\text{9}]\text{aneS}_3)(\text{dcpe})]^{2+}$ with numbering scheme adopted

isolable product. This reflects the high kinetic inertness and thermodynamic stability of the homoleptic hexathioether complexes of type $[\text{M}([\text{9}]\text{aneS}_3)_2]^{n+}$. Indeed, we have found that the formation of half-sandwich complexes of [9]aneS₃ of late first-row transition metal ions is severely hampered by formation of the bis(sandwich) species $[\text{M}([\text{9}]\text{aneS}_3)_2]^{2+}$.

The ¹H NMR spectra of $[\text{Ni}([\text{9}]\text{aneS}_3)(\text{L-L})]^{2+}$ in CD₃CN or CD₃NO₂ exhibit the resonances expected from one diphosphine ligand, as well as a symmetric multiplet centred at between δ 3.2 and 2.6 assigned to [9]aneS₃. Carbon-13 NMR spectroscopy shows, in addition to resonances due to the phosphine ligands, a single resonance in the region δ 35.2–36.5 consistent with a fluxional [9]aneS₃ ligand. No decoalescence of the [9]aneS₃ resonance for $[\text{Ni}([\text{9}]\text{aneS}_3)(\text{dppe})][\text{PF}_6]_2$ was observed down to 218 K in ²H₆acetone. Infrared spectroscopy of $[\text{Ni}([\text{9}]\text{aneS}_3)(\text{L-L})][\text{PF}_6]_2$ confirms the presence of

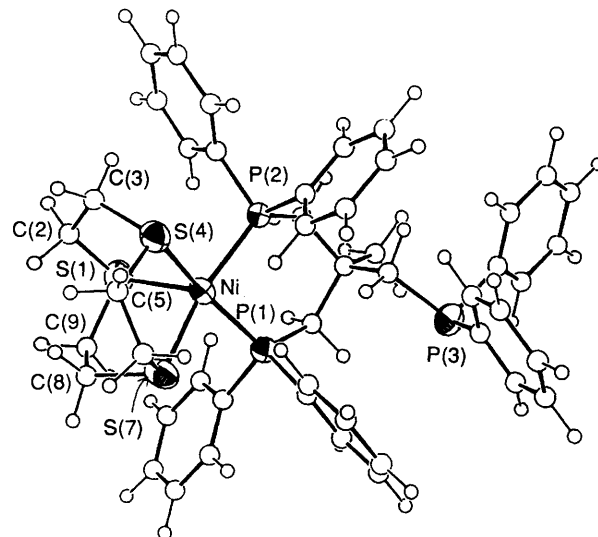


Fig. 3 Single-crystal structure of $[\text{Ni}([\text{9}]\text{aneS}_3)(\text{tdpm})]^{2+}$ with numbering scheme adopted

Table 1 Selected bond lengths (Å) and angles (°) with estimated standard deviations (e.s.d.s) for $[\text{Ni}([\text{9}]\text{aneS}_3)(\text{dppm})][\text{PF}_6]_2$

Ni–S(1)	2.4007(21)	P(1)–C(26)	1.785(5)
Ni–S(4)	2.2179(25)	P(1)–C(36)	1.802(5)
Ni–S(7)	2.2336(24)	P(2)–C(10)	1.823(7)
Ni–P(1)	2.1747(19)	P(2)–C(46)	1.781(5)
Ni–P(2)	2.1820(20)	P(2)–C(56)	1.789(7)
P(1)–C(10)	1.811(7)		
S(1)–Ni–S(4)	91.38(8)	Ni–S(7)–C(6')	103.2(6)
S(1)–Ni–S(7)	91.28(8)	Ni–S(7)–C(8')	100.0(6)
S(1)–Ni–P(1)	102.17(7)	C(6')–S(7)–C(8')	103.8(8)
S(1)–Ni–P(2)	104.08(7)	Ni–P(1)–C(26)	116.18(17)
S(4)–Ni–S(7)	91.77(9)	Ni–P(1)–C(36)	118.60(17)
S(4)–Ni–P(1)	164.26(9)	Ni–P(1)–C(10)	95.36(23)
S(4)–Ni–P(2)	96.09(8)	C(26)–P(1)–C(36)	106.93(22)
S(7)–Ni–P(1)	95.83(8)	C(26)–P(1)–C(10)	108.9(3)
S(7)–Ni–P(2)	162.52(8)	C(36)–P(1)–C(10)	110.0(3)
P(1)–Ni–P(2)	73.05(7)	P(1)–C(26)–C(21)	120.6(4)
Ni–S(1)–C(2)	99.1(4)	P(1)–C(26)–C(25)	119.3(4)
Ni–S(1)–C(9)	97.5(4)	P(1)–C(36)–C(31)	118.8(3)
C(2)–S(1)–C(9)	100.6(5)	P(1)–C(36)–C(35)	121.0(3)
Ni–S(4)–C(3)	100.7(4)	P(1)–C(10)–P(2)	91.0(3)
Ni–S(4)–C(5)	103.8(4)	Ni–P(2)–C(10)	94.77(23)
C(3)–S(4)–C(5)	100.8(6)	Ni–P(2)–C(46)	120.62(19)
Ni–S(7)–C(6)	100.5(4)	Ni–P(2)–C(56)	115.11(22)
Ni–S(7)–C(8)	103.0(3)	C(10)–P(2)–C(46)	107.6(3)
C(6)–S(7)–C(8)	99.9(5)	C(10)–P(2)–C(56)	112.0(3)
Ni–S(1)–C(2')	97.7(5)	C(46)–P(2)–C(56)	106.1(3)
Ni–S(1)–C(9')	98.7(5)	P(2)–C(46)–C(41)	121.0(4)
C(2')–S(1)–C(9')	99.8(7)	P(2)–C(46)–C(45)	119.0(4)
Ni–S(4)–C(3')	102.4(5)	P(2)–C(56)–C(51)	118.3(5)
Ni–S(4)–C(5')	100.3(6)	P(2)–C(56)–C(55)	121.2(5)
C(3')–S(4)–C(5')	97.9(8)		

Primed and unprimed equivalents define two different orientations of the [9]aneS₃ methylene groups. See Experimental section for details.

[9]aneS₃ and diphosphine ligands and PF₆⁻, and elemental analysis is consistent with the above stoichiometries. Electronic spectra of $[\text{Ni}([\text{9}]\text{aneS}_3)(\text{L-L})]^{2+}$ in MeCN are consistent with low-spin five-co-ordinate d⁸ nickel(II) centres,¹⁵ exhibiting two d-d bands at $\lambda_{\text{max}} = 500$ –600 and 415–450 nm, $\epsilon_{\text{max}} = 40$ –150 and 600–1800 dm³ mol⁻¹ cm⁻¹ respectively, which were assigned to the transitions ¹A₁ → ¹B₁ and ¹A₁ → ¹E respectively in C_{4v} symmetry. The third d-d transition expected for this geometry, ¹A₁ → ¹A₂, was not observed and is possibly obscured beneath charge-transfer bands at $\lambda_{\text{max}} = 325$ –280

Table 2 Selected bond lengths (\AA) and angles ($^\circ$) with e.s.d.s in parentheses for $[\text{Ni}([9]\text{janeS}_3)(\text{dcpe})][\text{PF}_6]_2 \cdot 1.25\text{MeCN}$

Ni-S(1)	2.6521(20)	C(6)-S(7)	1.868(8)
Ni-S(4)	2.2260(19)	S(7)-C(8)	1.962(8)
Ni-S(7)	2.2402(20)	C(8)-C(9)	1.501(11)
Ni-P(1)	2.1654(19)	P(1)-C(26)	2.038(7)
Ni-P(2)	2.2173(19)	P(1)-C(36)	1.808(7)
S(1)-C(2)	1.766(8)	P(1)-C(11)	1.857(7)
S(1)-C(9)	1.804(8)	C(11)-C(12)	1.447(9)
C(2)-C(3)	1.657(10)	C(12)-P(2)	1.803(7)
C(3)-S(4)	1.882(7)	P(2)-C(46)	1.815(7)
S(4)-C(5)	1.872(8)	P(2)-C(56)	2.030(7)
C(5)-C(6)	1.524(11)		
S(1)-Ni-S(4)	95.65(7)	S(1)-C(9)-C(8)	112.1(5)
S(1)-Ni-S(7)	89.06(7)	Ni-P(1)-C(26)	119.61(20)
S(1)-Ni-P(1)	102.66(7)	Ni-P(1)-C(36)	108.98(22)
S(1)-Ni-P(2)	116.98(7)	Ni-P(1)-C(11)	108.72(22)
S(4)-Ni-S(7)	84.95(7)	C(26)-P(1)-C(36)	109.4(3)
S(4)-Ni-P(1)	161.69(8)	C(26)-P(1)-C(11)	106.9(3)
S(4)-Ni-P(2)	87.46(7)	C(36)-P(1)-C(11)	101.7(3)
S(7)-Ni-P(1)	95.53(7)	P(1)-C(26)-C(21)	121.0(5)
S(7)-Ni-P(2)	153.50(8)	P(1)-C(26)-C(25)	116.1(5)
P(1)-Ni-P(2)	84.02(7)	P(1)-C(36)-C(31)	108.9(5)
Ni-S(1)-C(2)	93.4(3)	P(1)-C(36)-C(35)	116.1(4)
Ni-S(1)-C(9)	101.9(3)	P(1)-C(11)-C(12)	111.0(5)
C(2)-S(1)-C(9)	96.5(4)	C(11)-C(12)-P(2)	107.3(5)
S(1)-C(2)-C(3)	117.5(5)	Ni-P(2)-C(12)	112.61(23)
C(2)-C(3)-S(4)	118.9(5)	Ni-P(2)-C(46)	116.56(22)
Ni-S(4)-C(3)	99.97(23)	Ni-P(2)-C(56)	110.21(20)
Ni-S(4)-C(5)	108.32(24)	C(12)-P(2)-C(46)	97.7(3)
C(3)-S(4)-C(5)	104.3(3)	C(12)-P(2)-C(56)	107.3(3)
S(4)-C(5)-C(6)	105.3(5)	C(46)-P(2)-C(56)	111.6(3)
C(5)-C(6)-S(7)	110.4(5)	P(2)-C(46)-C(41)	117.7(4)
Ni-S(7)-C(6)	109.5(3)	P(2)-C(46)-C(45)	108.2(5)
Ni-S(7)-C(8)	101.35(24)	P(2)-C(56)-C(51)	118.8(5)
C(6)-S(7)-C(8)	106.7(3)	P(2)-C(56)-C(55)	115.3(5)
S(7)-C(8)-C(9)	121.2(5)		

(split into two bands for L-L = dcpe) and 266–243 nm, $\varepsilon_{\text{max}} = 6730\text{--}14\,630$ and $13\,190\text{--}28\,650\text{ dm}^3\text{ mol}^{-1}\text{ cm}^{-1}$ respectively.

Single crystals of $[\text{Ni}([9]\text{janeS}_3)(\text{dppm})][\text{PF}_6]_2$, $[\text{Ni}([9]\text{janeS}_3)(\text{dcpe})][\text{PF}_6]_2 \cdot 1.25\text{MeCN}$ and $[\text{Ni}([9]\text{janeS}_3)(\text{tdpme})][\text{PF}_6]_2$ were obtained by vapour diffusion of Et_2O into solutions of the complexes in MeCN. The single-crystal structures of these complexes (Figs. 1–3, Tables 1–3) confirm the presence of five-co-ordinate nickel(II) centres, and show them adopting distorted square-pyramidal geometries. The Ni–S and Ni–P bond lengths (Tables 1–3) vary significantly between the complexes, illustrating the differing steric demands of the diphosphine ligands: for $[\text{Ni}([9]\text{janeS}_3)(\text{dppm})]^{2+}$ Ni–S 2.2179(25), 2.2336(24), 2.4007(21) \AA , Ni–P 2.1747(19), 2.1820(20) \AA ; for $[\text{Ni}([9]\text{janeS}_3)(\text{dcpe})]^{2+}$ Ni–S 2.2260(19), 2.2402(20), 2.6521(20) \AA , Ni–P 2.1654(19), 2.2173(19) \AA ; for $[\text{Ni}([9]\text{janeS}_3)(\text{tdpme})]^{2+}$ Ni–S 2.242(5), 2.266(5), 2.458(5) \AA , Ni–P 2.214(4), 2.224(4) \AA ; cf. for $[\text{Ni}([9]\text{janeS}_3)(\text{dppe})]^{2+}$ Ni–S_{av} 2.226(3), 2.246(3), 2.390(3) \AA , Ni–P_{av} 2.190(3), 2.191(3) \AA .¹⁶ The Ni atom lies 0.262, 0.422 and 0.318 \AA above the least-squares basal planes of the $[\text{Ni}([9]\text{janeS}_3)(\text{L-L})]^{2+}$ complex cations for L-L = dppm, dcpe and tdpme respectively. The S_2P_2 basal plane for $[\text{Ni}([9]\text{janeS}_3)(\text{dcpe})]^{2+}$ exhibits a significant tetrahedral distortion, with S(4), S(7), P(1) and P(2) lying +0.085, -0.080, +0.083 and -0.087 \AA from the least-squares basal plane respectively: it is unclear whether this is a result of steric interactions between the dcpe cyclohexyl substituents and macrocyclic methylene groups, or whether it reflects an electronic distortion of the type recently proposed for four-co-ordinate $[\text{Ni}(\text{L-L})_2]^{2+}$ [L-L = bis(diphenylphosphino)chelate].¹⁷ The S–Ni–S angles for all three complexes lie between 89.0 and 91.8°. The related d⁸ complexes $[\text{Pd}([9]\text{janeS}_3)\text{L}_2]^{2+}$ ($\text{L}_2 = 2\text{PPh}_3$, dppm, oxy-tdpme, bipy or phen) and $[\text{Pt}([9]\text{janeS}_3)(\text{dppm})]^{2+}$ also exhibit square-

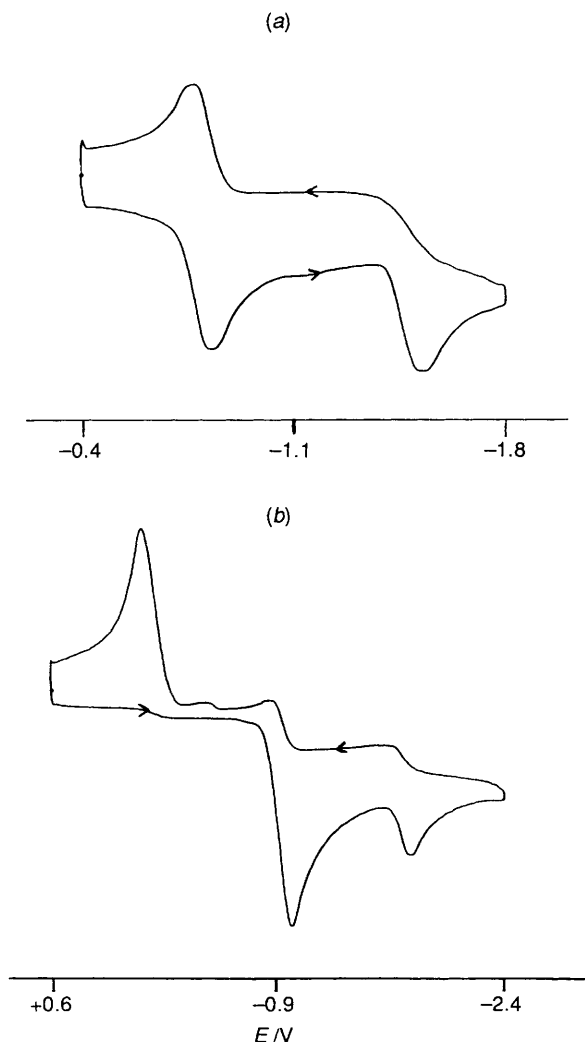


Fig. 4 Cyclic voltammogram of $[\text{Ni}([9]\text{janeS}_3)(\text{dppe})][\text{PF}_6]_2$ in MeCN ($0.1\text{ mol dm}^{-3}\text{ NBu}_4\text{PF}_6$) at 293 K , scan rate 400 mV s^{-1} ; (a) under Ar, (b) under CO

pyramidal stereochemistries in the solid state, with unusually short apical M–S (M = Pd or Pt) distances of $2.7\text{--}2.9\text{ \AA}$.¹⁸

Cyclic voltammetry of $[\text{Ni}([9]\text{janeS}_3)(\text{L-L})][\text{PF}_6]_2$ in MeCN ($0.1\text{ mol dm}^{-3}\text{ NBu}_4\text{PF}_6$) at 293 K shows one chemically reversible and one quasi-reversible reduction (Table 4, Fig. 4), assigned to $\text{Ni}^{\text{II}}\text{-}\text{Ni}^{\text{I}} [\text{Ni}([9]\text{janeS}_3)(\text{L-L})]^{2+/+}$ and $\text{Ni}^{\text{I}}\text{-}\text{Ni}^{\text{O}} [\text{Ni}([9]\text{janeS}_3)(\text{L-L})]^{+/0}$ couples respectively. Very importantly, coulometric measurements confirm all these processes to be one-electron processes. Interestingly, the cyclic voltammetric wave for the couple $[\text{Ni}([9]\text{janeS}_3)(\text{tdpme})]^{2+/+}$ exhibits a double return wave: given the reversibility and isosbesticity of this redox process (see below), this was taken to indicate partial adsorption of the complex onto the Pt electrodes via the dangling tdpme P-donor, or, more likely, the formation on the cyclic voltammetric time-scale of redox products of different connectivities.

Controlled-potential electroreduction of the complexes $[\text{Ni}([9]\text{janeS}_3)(\text{L-L})][\text{PF}_6]_2$ in MeCN ($0.1\text{ mol dm}^{-3}\text{ NBu}_4\text{PF}_6$) at 293 K (L-L = dppe, dppv, dppm or tdpme) and 253 K (L-L = dppm, dcpe or dmpe) at a potential corresponding to an overall one-electron reduction affords products, the solution ESR spectra of which all show triplet resonances due to coupling of the unpaired electron to two equivalent P atoms. This confirms that both P-donors remain co-ordinated to the nickel(I) centre in the one-electron reduction product. At 77 K , axial or rhombic ESR spectra are observed [Figs. 5 and 6(a), Table 5]. The ESR spectra as frozen glasses at 77 K were interpreted and simulated

assuming equal hyperfine coupling to both ^{31}P nuclei of the phosphine ligands: in cases of axial symmetry, the expected pattern $g_{\parallel} > g_{\perp}$ is observed, implying a $d_{x^2-y^2}$ ground state.¹⁹ The hyperfine coupling constants to ^{31}P for $[\text{Ni}([9]\text{aneS}_3)(\text{L-L})]^+$ are significantly greater than those observed by Bowmaker *et al.*²⁰ for the square planar $[\text{Ni}(\text{E-E})(\text{L-L})]^{n-}$ [E-E = dithiocarbamate, 1,2-dithiole or 1,3-dithio- β -diketone, L-L = bis(diphenylphosphino) chelate].²⁰

Table 3 Selected bond lengths (\AA) and angles ($^{\circ}$) with e.s.d.s in parentheses for $[\text{Ni}([9]\text{aneS}_3)(\text{tdpme})][\text{PF}_6]_2$

Ni-S(1)	2.458(5)	P(1)-C(26)	1.802(11)
Ni-S(4)	2.266(5)	P(1)-C(36)	1.824(10)
Ni-S(7)	2.242(5)	P(1)-C(13)	1.813(16)
Ni-P(1)	2.224(4)	P(2)-C(46)	1.808(11)
Ni-P(2)	2.214(4)	P(2)-C(56)	1.817(10)
S(1)-C(2)	1.827(21)	P(2)-C(14)	1.792(14)
S(1)-C(9)	1.778(18)	P(3)-C(66)	1.817(12)
C(2)-C(3)	1.46(3)	P(3)-C(76)	1.868(12)
C(3)-S(4)	1.849(19)	P(3)-C(15)	1.860(16)
S(4)-C(5)	1.787(19)	C(11)-C(12)	1.536(22)
C(5)-C(6)	1.49(3)	C(12)-C(13)	1.573(21)
C(6)-S(7)	1.819(20)	C(12)-C(14)	1.533(20)
S(7)-C(8)	1.850(21)	C(12)-C(15)	1.533(21)
C(8)-C(9)	1.52(3)		
S(1)-Ni-S(4)	88.99(16)	P(1)-C(26)-C(21)	119.1(8)
S(1)-Ni-S(7)	89.40(16)	P(1)-C(26)-C(25)	120.8(8)
S(1)-Ni-P(1)	107.69(16)	P(1)-C(36)-C(31)	120.9(7)
S(1)-Ni-P(2)	105.90(16)	P(1)-C(36)-C(35)	118.9(7)
S(4)-Ni-S(7)	89.27(16)	Ni-P(2)-C(46)	110.9(4)
S(4)-Ni-P(1)	162.71(17)	Ni-P(2)-C(56)	113.7(3)
S(4)-Ni-P(2)	88.56(16)	Ni-P(2)-C(14)	118.7(5)
S(7)-Ni-P(1)	86.48(16)	C(46)-P(2)-C(56)	105.3(5)
S(7)-Ni-P(2)	164.50(16)	C(46)-P(2)-C(14)	99.7(6)
P(1)-Ni-P(2)	91.07(15)	C(56)-P(2)-C(14)	106.9(6)
Ni-S(1)-C(2)	101.6(7)	P(2)-C(46)-C(41)	121.1(8)
Ni-S(1)-C(9)	98.9(6)	P(2)-C(46)-C(45)	118.9(8)
C(2)-S(1)-C(9)	110.7(9)	P(2)-C(56)-C(51)	121.7(7)
S(1)-C(2)-C(3)	117.6(14)	P(2)-C(56)-C(55)	118.3(7)
C(2)-C(3)-S(4)	116.6(14)	C(66)-P(3)-C(76)	100.6(5)
Ni-S(4)-C(3)	104.4(6)	C(66)-P(3)-C(15)	101.4(6)
Ni-S(4)-C(5)	105.1(6)	C(76)-P(3)-C(15)	101.6(6)
C(3)-S(4)-C(5)	105.1(8)	P(3)-C(66)-C(61)	115.4(8)
S(4)-C(5)-C(6)	115.0(13)	P(3)-C(66)-C(65)	124.5(8)
C(5)-C(6)-S(7)	112.4(13)	P(3)-C(76)-C(71)	115.5(8)
Ni-S(7)-C(6)	102.4(6)	P(3)-C(76)-C(75)	124.5(8)
Ni-S(7)-C(8)	105.7(7)	C(11)-C(12)-C(13)	106.2(12)
C(6)-S(7)-C(8)	100.6(9)	C(11)-C(12)-C(14)	107.8(12)
S(7)-C(8)-C(9)	111.4(13)	C(11)-C(12)-C(15)	110.0(12)
S(1)-C(9)-C(8)	116.8(13)	C(13)-C(12)-C(14)	109.3(12)
Ni-P(1)-C(26)	113.0(4)	C(13)-C(12)-C(15)	109.7(12)
Ni-P(1)-C(36)	108.1(4)	C(14)-C(12)-C(15)	113.5(12)
Ni-P(1)-C(13)	122.4(5)	P(1)-C(13)-C(12)	119.4(11)
C(26)-P(1)-C(36)	105.4(5)	P(2)-C(14)-C(12)	119.9(10)
C(26)-P(1)-C(13)	105.2(6)	P(3)-C(15)-C(12)	115.7(10)
C(36)-P(1)-C(13)	101.0(6)		

Table 4 Summary of electrochemical data for $[\text{Ni}([9]\text{aneS}_3)(\text{L-L})][\text{PF}_6]_2$ complexes

L-L	Oxidation		1st reduction			2nd reduction		
	E ^a /V	n ^b	E ^a /V	n ^b	$\Delta E_p/\text{mV}$	E ^a /V	Total n ^b	$\Delta E_p/\text{mV}$
dppm	—	—	-0.77(r)	0.90	91	-1.50(i)	1.99	—
dppe	—	—	-0.88(r)	1.03	64	-1.65(i)	1.91	—
dppv	—	—	-0.82(r)	0.93	61	-1.59(i)	2.08	—
dcpe	—	—	-0.96(r)	0.98	84	-1.84(i)	—	—
dmpe	+1.22(i) ^c	0.95	-1.16(r)	0.96	72	-1.93(i)	—	—
dppp	—	—	-0.79(r)	1.00	92	-1.63(i)	1.91	—
tdpme	+1.04(i)	0.91	-0.77(q)	1.08	d	-1.31(q)	1.94	71

^a Electrochemical redox potential, measured at 298 K, in MeCN-0.1 mol dm⁻³ NBu₄PF₆, scan rate 400 mV s⁻¹, under an argon atmosphere. Potentials quoted vs. ferrocene-ferrocenium; r = chemically reversible, q = quasi-reversible, i = irreversible. ^b n = Number of moles of electrons transferred in oxidation (reduction) of 1 mole of complex (coulometric determination). ^c Exhibits a return wave at E_p = +0.21 V. ^d Exhibits two return waves.

Chemical reduction of $[\text{Ni}([9]\text{aneS}_3)(\text{L-L})][\text{PF}_6]_2$ (L-L = dppe, dppv, dcpe, dppp or tdpme) with NaBH₄ in MeOH under N₂ at 293 K gives the same coloured solutions which exhibit identical ESR and electronic spectra to those of the electro-reduced samples. Thus, these nickel(I) products can be readily generated by chemical as well as electrochemical reduction.

In order to quantify the electronic character of complexes of type $[\text{Ni}([9]\text{aneS}_3)(\text{L-L})]^+$, the ESR spectroscopy of a 62% ⁶¹Ni-enriched sample of $[\text{Ni}([9]\text{aneS}_3)(\text{tdpme})]^+$ was examined. The ESR spectrum of this enriched species in MeCN (0.1 mol dm⁻³ NBu₄PF₆) and in MeOH solutions at 293 K shows a triplet of four lines, with $g_{\text{iso}} = 2.095$, $A_{\text{iso}}(^{31}\text{P}) = 126$ G, $A_{\text{iso}}(^{61}\text{Ni}, I = \frac{3}{2}) = 21$ G, whilst at 77 K the additional hyperfine coupling to ⁶¹Ni is resolvable at $A_{\parallel} = 53$ G, $A_{\perp} = 8$ G (Fig. 6). For a $S = \frac{1}{2}$ radical with a $d_{x^2-y^2}$ ground state, the hyperfine coupling to the metal nucleus can be described by equations (1) and (2),^{21,22} where K is the Fermi contact term for isotropic

$$A_{\parallel} = -K + P_0[(-\frac{4}{7})\alpha^2 + (g_{\parallel} - g_e) + \frac{3}{7}(g_{\perp} - g_e)] \quad (1)$$

$$A_{\perp} = -K + P_0[(\frac{2}{7})\alpha^2 + \frac{11}{14}(g_{\perp} - g_e)] \quad (2)$$

hyperfine coupling to the metal nucleus, P_0 is the coupling constant for dipole-dipole coupling to the free metal ion ($P_0 = 102$ G for ⁶¹Ni²³) and α^2 is a covalency factor that gives the reduction in the observed dipole-dipole coupling from the free ion value P_0 , i.e. $\alpha^2 = 1$ for purely ionic metal-ligand bonding, $\alpha^2 < 1$ in the presence of metal-ligand covalency. Solving these

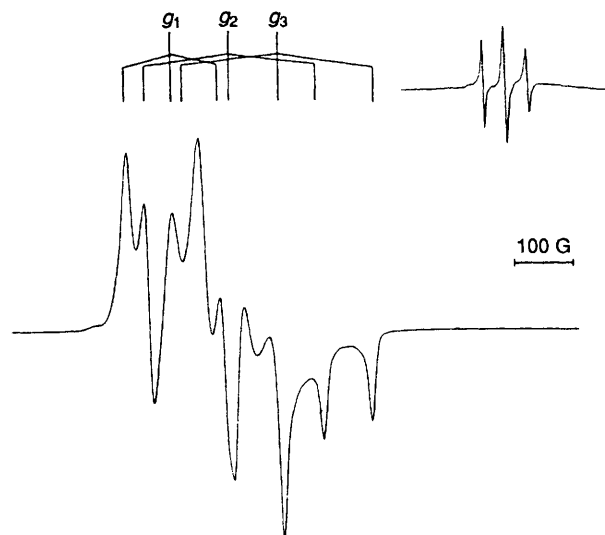


Fig. 5 ESR spectrum of $[\text{Ni}([9]\text{aneS}_3)(\text{dcpe})]^+$ in MeCN (0.1 mol dm⁻³ NBu₄PF₆) at 77 K, inset isotropic spectrum in MeOH at 293 K

Table 5 ESR data for $[\text{Ni}([\text{9}]\text{aneS}_3)(\text{L-L})]^+$

L-L	Colour of solution	Mobile solution ^a		Frozen glass ^b					
		g_{iso}	$A_{\text{iso}}/\text{G}^c$	g_1	A_1/G^c	g_2	A_2/G^c	g_3	A_3/G^c
dppm	Orange	2.110	127*	2.193	98	2.098	149	2.041	167
dppe	Dark red	2.086	118	2.136	98	2.051	111	2.051	152
dppv	Dark red	2.086	118	2.141	98	2.063	122	2.053	147
dcpe	Yellow	2.104	107	2.167	80	2.107	127	2.037	133
dmpe	Green	2.090	127*	2.149	94	2.090	149	2.042	174
dppp	Orange	2.098	120	2.158	120	2.060	132		
tdpme ^d	Orange	2.095	126	2.154	126	2.060	137		

^aSolution spectra measured at 298 K in CH_3OH except * in MeCN (0.1 mol dm^{-3} NBu_4PF_6). ^bFrozen glass spectra measured at 77 K in MeCN (0.1 mol dm^{-3} NBu_4PF_6). ^cHyperfine coupling to ^{31}P . ^dHyperfine constants to ^{61}Ni ($I = \frac{3}{2}$) $A_{\text{iso}} = 21 \text{ G}$, $A_1 = 53 \text{ G}$, $A_2, A_3 = 8 \text{ G}$.

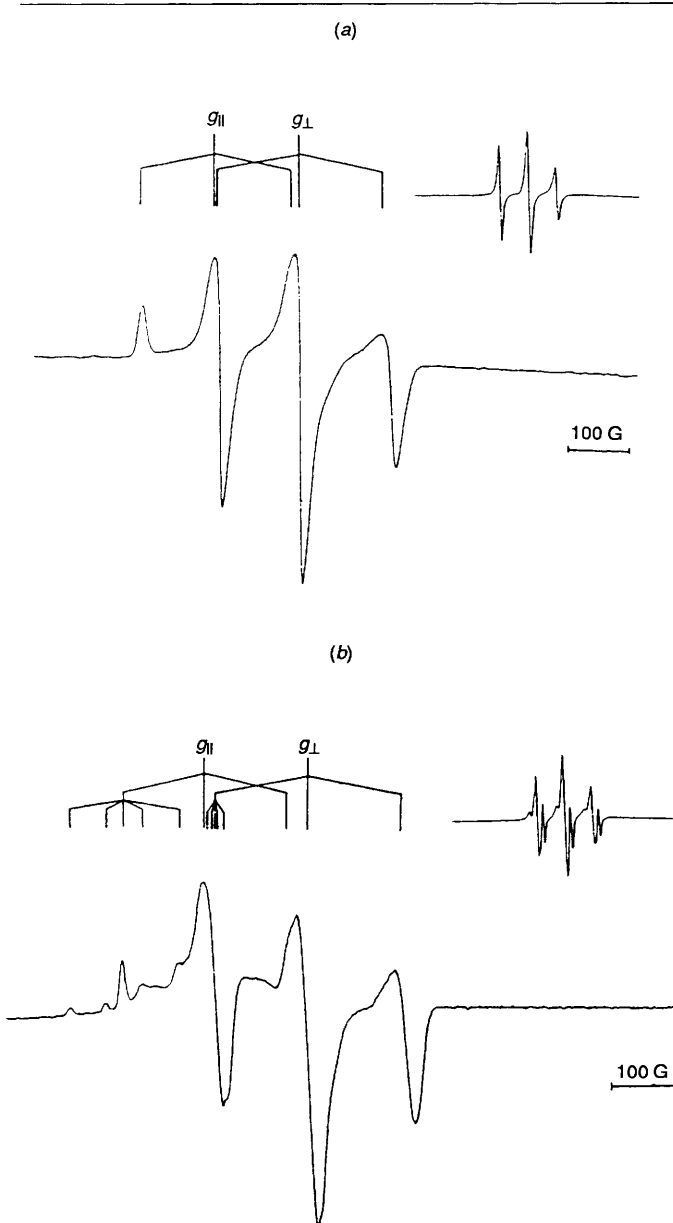


Fig. 6 ESR spectra of $[\text{Ni}([\text{9}]\text{aneS}_3)(\text{tdpme})]^+$ in MeCN (0.1 mol dm^{-3} NBu_4PF_6) at 77 K; (a) unenriched sample, (b) 62%-enriched with ^{61}Ni ($I = \frac{3}{2}$)

equations using $g_{\parallel} = 2.154$, $A_{\parallel} = -53 \text{ G}$, $g_{\perp} = 2.060$, $A_{\perp} = -8 \text{ G}$ gives $\alpha^2 = 0.67$ for $[\text{Ni}([\text{9}]\text{aneS}_3)(\text{tdpme})]^+$. While clearly consistent with a metal-based radical, this covalency factor is significantly lower than for other nickel(i) complexes;

for example, for $[\text{Ni}(\text{tmc})]^+$ ($\text{tmc} = 1,4,8,11\text{-tetramethyl-1,4,8,11-tetraazacyclotetradecane}$) $\alpha^2 = 0.74$,²⁴ for $[\text{Ni}(\text{tpo})_2]^-$ ($\text{Htpo} = 2\text{-thioxopyridine N-oxide}$) $\alpha^2 = 0.87$,²⁵ while for $[\text{Ni}(\text{mnt})_2]^-$ ($\text{H}_2\text{mnt} = 2,3\text{-dimercaptomaleonitrile}$) $\alpha^2 = 0.70$ or 0.85 .^{21,22} This reflects the five-co-ordination, the π -acceptor properties of the ligands, and the monopositive charge in $[\text{Ni}([\text{9}]\text{aneS}_3)(\text{L-L})]^+$. Interestingly, all other nickel(i) complexes characterised in this way have had square-planar geometries.

The reductions of $[\text{Ni}([\text{9}]\text{aneS}_3)(\text{L-L})]^2+$ to $[\text{Ni}([\text{9}]\text{aneS}_3)(\text{L-L})]^+$ were monitored spectroelectrochemically using an optically transparent electrode (ote) system (Table 6, Fig. 7). Importantly, for L-L = dppe, dppv, dcpe, dmpe, dppp and tdpme this reduction proceeds isosbastically and is quantitatively reversible at both 253 and 243 K when L-L = dmpe (Table 6). The electronic spectra of $[\text{Ni}([\text{9}]\text{aneS}_3)(\text{L-L})]^+$ (L-L = dppe, dppv, dmpe, dppp or tdpme) exhibit two d-d bands, at $\lambda_{\text{max}} = 512\text{--}350$ and $398\text{--}308 \text{ nm}$, $\epsilon_{\text{max}} = 1250\text{--}1760$ and $1545\text{--}2060 \text{ dm}^3 \text{ mol}^{-1} \text{ cm}^{-1}$ respectively: it is possible that these bands may be obscured in $[\text{Ni}([\text{9}]\text{aneS}_3)(\text{dcpe})]^+$ by the additional charge-transfer band shown by this complex. The wide variation in the energies of these d-d bands for different diphosphine ligands is consistent with the observed $d_{x^2-y^2}$ ground state for $[\text{Ni}([\text{9}]\text{aneS}_3)(\text{L-L})]^+$, and accounts for their differing colours. In general, the nickel(i) complexes show charge-transfer bands of reduced intensity compared to the parent nickel(II) species. However, the behaviour of these absorptions varies between the complexes and prevents their unambiguous assignment. The reduction of $[\text{Ni}([\text{9}]\text{aneS}_3)(\text{dppm})]^2+$ to $[\text{Ni}([\text{9}]\text{aneS}_3)(\text{dppm})]^+$ is not isosbestic at 253 K, although the final nickel(i) absorption spectrum is similar to those exhibited by the other complexes in the series (Table 6) and re-oxidation at 0.0 V quantitatively regenerates the nickel(II) cation. This may reflect isomerism in the reduced species between five-co-ordinate and tetrahedral geometries via de-co-ordination of one P-donor caused by the strain associated with the four-membered chelate ring.

The above cyclic voltammetric, ESR and electronic spectral data are consistent with the formation of five-co-ordinate, square-pyramidal d^9 cations $[\text{Ni}([\text{9}]\text{aneS}_3)(\text{L-L})]^+$. The geometries adopted by these species should be similar to those observed for the nickel(II) precursors. The geometry of nickel(i) centres appears to be dominated by the imposed ligand co-ordination sphere. Thus, square-pyramidal,^{3,26} square-planar,²⁷ tetrahedral and trigonal-bipyramidal^{28,29} and trigonal-planar co-ordination³⁰ have all been observed for nickel(ii) complexes, the geometry at the metal centre being dictated by the stereochemical requirements of the ligands used; i.e. square-planar nickel(i) complexes tend to be of tetradentate planar macrocycles,²⁷ square-pyramidal species tend to be 1:1 adducts of square-planar macrocyclic complexes,³ while trigonal-bipyramidal nickel(i) species contain tripodal ligands.^{28,29} In the case of the complexes $[\text{Ni}([\text{9}]\text{aneS}_3)(\text{L-L})]^+$, five-co-ordination is imposed by the ligand set. Related trigonal-bipyramidal complexes of [9]aneS₃ such as

Table 6 UV/VIS spectral data [λ_{max} /nm (ϵ_{max} /dm³ mol⁻¹ cm⁻¹)] for $[\text{Ni}([\text{9}]\text{aneS}_3)(\text{L-L})]^{2+/+0a}$

L-L	Ni ^{II}	Ni ^{II} -Ni ^I (λ_{iso})	Ni ^I	Ni ⁰
dppm	418 (2130), 320 (14 880), 266 (13 715)	—	460 (sh), 408 (2420) 319 (9800), 265 (13 150)	466 (sh), 395 (sh), 320 (sh), 265 (10 610)
dppe	422 (1650), 316 (17 390), 266 (13 070)	343, 284, 278, 260	512 (1580), 398 (2060), 327 (7300), 262 (11 840)	460 (sh), 319 (sh), 262 (9470)
dppv	420 (2320), 318 (18 340), 260 (19 190)	445, 412, 350, 293, 273	514 (1740), 395 (2220), 325 (9200), 266 (sh)	482 (sh), 380 (sh), 320 (sh), 265 (16 850)
dcpe	435 (835), 325 (7015), 292 (12 990), 243 (14 580)	398, 344, 272, 256, 217	320 (4220), 287 (8580), 249 (12 590)	—
dmpe*	413 (650), 283 (13 350), 244 (12 740)	394, 316	350 (1760), 308 (sh), 267 (sh), 244 (10 650)	—
dppp	452 (1250), 329 (11 270), 260 (10 480)	365, 293	477 (1250), 398 (1545), 319 (7830), 263 (10 880)	462 (sh), 398 (sh), 323 (sh), 262 (10 050)
tdpme	443 (1860), 328 (14 640), 260 (18 710)	478, 420, 364, 293, 272	488 (1250), 380 (sh), 322 (8270), 260 (17 090)	386 (7725), 328 (8600), 260 (14 290)

* All spectra recorded in optically transparent electrode cell in MeCN (0.1 mol dm⁻³ NBu₄PF₆) at 253 K except * 243 K.

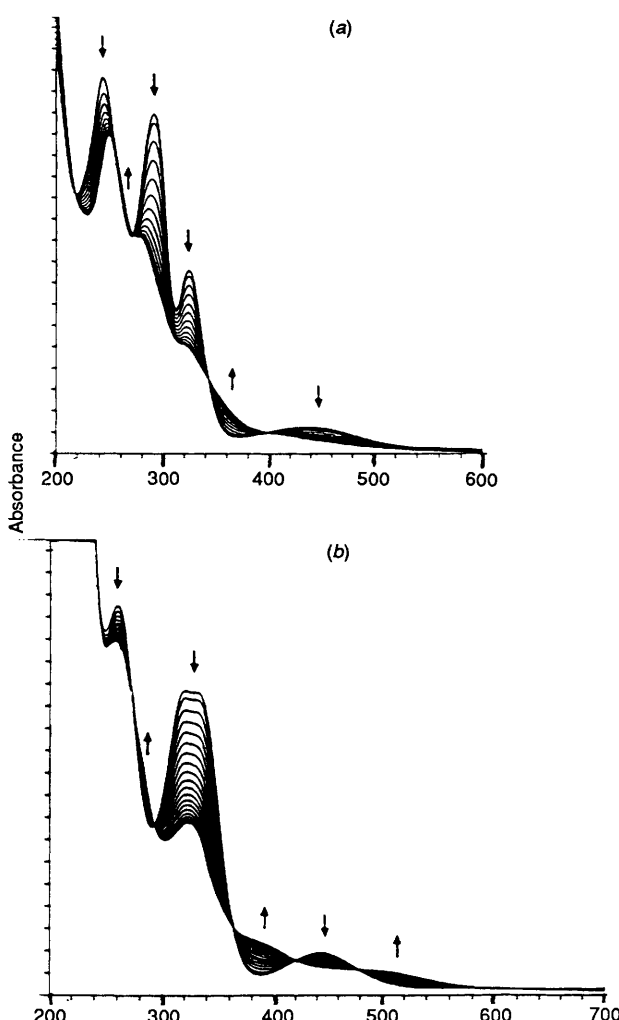
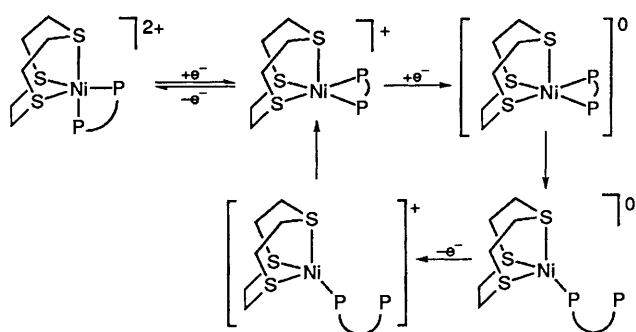


Fig. 7 Reduction of $[\text{Ni}([\text{9}]\text{aneS}_3)(\text{L-L})]^{2+}$ to $[\text{Ni}([\text{9}]\text{aneS}_3)(\text{L-L})]^+$ by controlled potential electrolysis in MeCN (0.1 mol dm⁻³ NBu₄PF₆) at 253 K; (a) L-L = dcpe, (b) L-L = tdpme

$[\text{Rh}([\text{9}]\text{aneS}_3)(\text{cod})]^+$ (cod = cycloocta-1,5-diene) have been reported previously.³¹

Controlled-potential electrolysis of $[\text{Ni}([\text{9}]\text{aneS}_3)(\text{L-L})]\text{PF}_6^2$ (L-L = dppm, dppe, dppv, dppp or tdpme) in MeCN (0.1 mol dm⁻³ NBu₄PF₆) at 243 K at potentials beyond the second reduction couple affords yellow ESR-silent solutions. Monitoring the reductions of $[\text{Ni}([\text{9}]\text{aneS}_3)(\text{L-L})]^+$ to



Scheme 1 Proposed stereochemical changes on reduction of five-coordinate $[\text{Ni}([\text{9}]\text{aneS}_3)(\text{L-L})]^{2+}$ to five-coordinate nickel(i) and tetrahedral nickel(0) species

$[\text{Ni}([\text{9}]\text{aneS}_3)(\text{L-L})]^0$ using the ote system shows that they do not proceed isosbistically, and that reduction is accompanied by collapse of the d-d bands of the nickel(i) spectrum resulting in spectra containing only broad charge-transfer bands (Table 6). Consistent with the cyclic voltammetric measurements, re-oxidation at potentials between the two redox couples only gives partial regeneration of $[\text{Ni}([\text{9}]\text{aneS}_3)(\text{L-L})]^+$: however, re-oxidation at 0.0 V results in quantitative regeneration of the initial nickel(ii) precursors (except for L-L = dppm). These data imply the formation of $d^{10} [\text{Ni}([\text{9}]\text{aneS}_3)(\text{L-L})]^0$, which should adopt a tetrahedral stereochemistry probably with one dangling P-donor (Scheme 1). Re-oxidation to $[\text{Ni}([\text{9}]\text{aneS}_3)(\text{L-L})]$ would then have to involve re-arrangement of tetrahedral nickel(0) to five-coordinate nickel(i), which would be expected to be slower than the corresponding reduction of five-coordinate d^9 nickel(i) to tetrahedral Ni⁰. Interestingly, the $[\text{Ni}([\text{9}]\text{aneS}_3)(\text{tdpme})]^{+0}$ couple occurs at a markedly less cathodic potential than the others in the series and exhibits a better defined return wave; the electronic spectrum of $[\text{Ni}([\text{9}]\text{aneS}_3)(\text{tdpme})]^0$ also shows an additional intense charge transfer band at $\lambda_{\text{max}} = 386 \text{ nm}$, $\epsilon_{\text{max}} = 7725 \text{ dm}^3 \text{ mol}^{-1} \text{ cm}^{-1}$. We suggest that the third tdpme P-donor may co-ordinate to the nickel atom on reduction to nickel(0) giving a tetrahedral geometry containing a monodentate [9]aneS₃ ligand. Stabilisation of nickel(0) would thereby be enhanced by co-ordination to three π -acceptor P-donors rather than three weaker π -acceptor thioether S-donors; moreover, monodentate co-ordination of [9]aneS₃ has been observed previously in d^{10} copper(i)³² and gold(i)^{12,13} complexes of this ligand. Attempted generation of $[\text{Ni}([\text{9}]\text{aneS}_3)(\text{L-L})]^0$ (L-L = dcpe, dmpe) by controlled potential electrolysis under identical conditions gives colourless ESR-silent solutions, with deposition of nickel metal onto the Pt working electrode: no current flow was observed on attempted re-oxidation of these solutions at 0.0 V.

Table 7 Summary of electrochemical data for $[\text{Ni}(\text{[9]aneS}_3)(\text{L-L})]\text{[PF}_6\text{]}_2$ complexes under a CO atmosphere

L-L	E (1st reduction) ^a /V	E (2nd reduction) ^a /V	E (Return oxidation) ^a /V
dppm	-0.77(i)	—	-0.03(i,w)
dppe	-0.88(q)	-1.76(i,w)	0.00(i)
dppv	-0.80(q)	-1.65(i,w)	+0.02(i)
dcpe	-0.98(i)	—	-0.11(i)
dmpe	-1.14(i)	—	-0.19(i)
dppp	-0.78(i)	-1.76(i,w)	-0.07(i)
tdpme	-0.80(i)	—	-0.32(i), +0.05(i)

^a Electrochemical redox potential measured at 298 K, in MeCN (0.1 mol dm⁻³ NBu₄PF₆), scan rate 400 mV s⁻¹, under a CO atmosphere. Potentials quoted vs. ferrocene–ferrocenium; q = quasi-reversible, i = irreversible, w = weak.

In addition to the reductive processes described above, the cyclic voltammograms of $[\text{Ni}(\text{[9]aneS}_3)(\text{dmpe})]\text{[PF}_6\text{]}_2$ and $[\text{Ni}(\text{[9]aneS}_3)(\text{tdpme})]\text{[PF}_6\text{]}_2$ exhibit an additional one-electron oxidation at $E_{p_e} = +1.22$ V (irreversible, return wave at $E_{p_e} = +0.21$ V) and at $E_{p_e} = +1.04$ V vs. ferrocene–ferrocenium (irreversible) respectively (Table 4). Controlled-potential electrolysis of $[\text{Ni}(\text{[9]aneS}_3)(\text{dmpe})]^{2+}$ at +1.45 V affords green solutions, which exhibit axial ESR spectra at 77 K that surprisingly show hyperfine coupling to two equivalent ¹⁴N nuclei, $g_{\perp} = 2.120$, $g_{\parallel} = 2.023$, $A_{\parallel} = 19$ G; $g_{\text{iso}} = 2.098$, $A_{\text{iso}} = 18$ G at 293 K. Chemical oxidation of $[\text{Ni}(\text{[9]aneS}_3)(\text{dmpe})]^{2+}$ in 70% HClO₄ or 98% H₂SO₄ gives dark red solutions, which exhibit ESR spectra with $g_{\perp} = 2.153$, $g_{\parallel} = 2.018$, $g_{\text{iso}} = 2.117$. These data suggest the formation of a d⁷ oxidation product, possibly with a square-planar or distorted octahedral geometry (the red species), which, in the electrochemical experiment co-ordinates two axial MeCN ligands to give species of the type $[\text{Ni}(\text{[9]aneS}_3)(\text{dmpe})(\text{NCMe})_2]^{3+}$ containing a bidentate [9]aneS₃ ligand. This mode of coordination is unusual for [9]aneS₃ but has been observed in $[\text{Ir}(\text{[9]aneS}_3)_2\text{H}]^{2+}$.³³ Controlled potential electrolysis of $[\text{Ni}(\text{[9]aneS}_3)(\text{tdpme})]^{2+}$ under identical conditions at +1.25 V proceeds slowly, and affords ESR-silent solutions identical in colour to the precursor complex. This process was therefore assigned as an oxidation of the dangling P-donor of the tdpme ligand, initially to a phosphonium radical cation which then reacts further to give an unknown final product. The oxidation of tertiary phosphines under aerobic conditions is well known.³⁴

A preliminary investigation of the reactivity of $[\text{Ni}(\text{[9]aneS}_3)(\text{L-L})]^+$ has been undertaken. Under a CO atmosphere, the Ni^{II}–Ni^I couple for $[\text{Ni}(\text{[9]aneS}_3)(\text{L-L})]\text{[PF}_6\text{]}_2$ becomes quasi-reversible or irreversible by cyclic voltammetry in MeCN (0.1 mol dm⁻³ NBu₄PF₆) at 293 K, and an additional return wave is observed at $E_{p_e} = -0.19$ to +0.05 V vs. ferrocene–ferrocenium, $i_{p_e}/i_{p_c} = 0.3$ –0.7 [Fig. 4(b), Table 7]. No diminution of the reduction or return waves is observed after 10 repeated cycles. Controlled potential electrolysis of $[\text{Ni}(\text{[9]aneS}_3)(\text{L-L})]^{2+}$ under CO at 293 K gives continuous current flow, with no change in colour of the solution; at 243 K, pale green or colourless solutions result, from which a weak ESR signal with $g_{\parallel} = 2.093$, $g_{\perp} = 2.015$ could sometimes be detected. These data imply the formation of an unstable adduct $[\text{Ni}(\text{[9]aneS}_3)(\text{L-L})(\text{CO})]^+$ which can be reoxidised to $[\text{Ni}(\text{[9]aneS}_3)(\text{L-L})]^{2+}$ at 293 K. No reaction is observed between $[\text{Ni}(\text{[9]aneS}_3)(\text{L-L})]^+$ and CO₂ by cyclic voltammetry. Current work is aimed at further characterisation of the $[\text{Ni}(\text{[9]aneS}_3)(\text{L-L})]^{+/\text{0}}$ redox species, and their reactions with CO and other small-molecule and organic substrates.

Experimental

Infrared spectra were run as KBr discs using a Perkin Elmer 598 spectrometer over the range 200–4000 cm⁻¹. Fast atom bombardment (FAB) mass spectra were obtained on a Kratos MS 50TC spectrometer using a 3-nitrobenzyl alcohol matrix. Micro-analyses were performed by the Edinburgh University Chemistry Department Microanalytical Service. Proton and ¹³C NMR spectra were recorded at 200.13 and 50.32 MHz respectively on a Bruker WP200 spectrometer, ³¹P NMR spectra on a JEOL FX90Q spectrometer operating at 36.23 MHz; ³¹P resonances due to PF₆⁻ have not been quoted. Electrochemical measurements were performed on Bruker E310 and EI30M Modular Polarographs. All readings were taken using a three-electrode potentiostatic system in MeCN containing 0.1 mol dm⁻³ NBu₄PF₆ as supporting electrolyte. Cyclic voltammetric measurements were carried out using a double platinum electrode and a Ag–AgCl reference electrode. All potentials are quoted *versus* ferrocene–ferrocenium. ESR spectra were recorded as mobile solutions or as frozen glasses down to 77 K using a Bruker ER200D X-band spectrometer. Electronic spectra were measured in 1 cm quartz cells using a Perkin Elmer Lambda-9 spectrophotometer. Spectroelectrochemical measurements were carried out in a quartz cell (path length 0.5 mm) fitted with a fine platinum–rhodium gauze as a working electrode. The platinum auxiliary electrode and Ag–Ag⁺ reference electrode were fitted into a quartz extension attached to the cell, and were protected from the bulk solution by porous glass frits. The temperature of the cell was maintained and controlled by the passage of dry, pre-cooled nitrogen gas around the assembly, and monitored using a thermocouple and digital thermometer.

1,4,7-Triphenylcyclononane, bis(diphenylphosphino)methane, 1,2-bis(diphenylphosphino)ethane, *cis*-1,2-bis(diphenylphosphino)ethene, 1,3-bis(diphenylphosphino)propane and 1,1,1-tris(diphenylphosphinomethyl)ethane were purchased from Aldrich chemicals. 1,2-Bis(dicyclohexylphosphino)ethane and 1,2-bis(dimethylphosphino)ethane were purchased from Strem chemicals. 62%-Enriched ⁶¹Ni foil was purchased from Atomic Energy Research Establishment, Harwell, and converted to ⁶¹Ni(NO₃)₂·6H₂O by dissolution in the minimum volume of 70% w/w HNO₃, followed by crystallisation at 253 K. The complexes $[\text{Ni}(\text{L-L})\text{Cl}_2]$ (L-L = dppm, dppe, dppv, dmpe and dppp) were synthesised according to literature methods.¹⁴

Syntheses.— $[\text{Ni}(\text{dcpe})\text{Cl}_2]$. Nickel(II) dichloride hexahydrate (0.28 g, 1.2×10^{-3} mol) was dissolved in propan-2-ol–MeOH (2:1, 30 cm³), mixed with dcpe (0.50 g, 1.2×10^{-3} mol) dissolved in propan-2-ol (50 cm³), and the mixture refluxed for 2 h. The resultant orange precipitate was filtered off and washed with cold propan-2-ol. Yield 0.58 g, 87% (Found: C, 56.5; H, 8.8. Calc. for C₂₂H₄₈Cl₂NP₂: C, 56.6; H, 8.8%). IR spectrum: 2920, 2840, 2640, 1440, 1400, 1340, 1300, 1290, 1265, 1200, 1170, 1145, 1115, 1080, 1045, 1005, 915, 885, 860, 845, 815, 790, 750, 735, 670, 650, 535, 510, 485, 460, 440, 400, 370, 340 and 315 cm⁻¹. Mass spectrum (FAB): *m/z* 550 {calc. for [⁵⁸Ni(dcpe)Cl₂]⁺, 550}, 515 {calc. for [⁵⁸Ni(dcpe)Cl]⁺, 515} and 480 {calc. for [⁵⁸Ni(dcpe)]⁺, 480}, with correct isotopic distributions. ³¹P-^{{1}H} NMR (CDCl₃, 293 K, 36.23 MHz): δ 82.65 (s).

$[\text{Ni}(\text{tdpme})\text{Cl}_2]$. Method as for $[\text{Ni}(\text{dcpe})\text{Cl}_2]$, using tdpme (0.75 g, 1.2×10^{-3} mol). The product was an orange solid. Yield 0.74 g, 82% (Found: C, 64.9; H, 5.2. Calc. for C₄₁H₃₉Cl₂NiP₂: C, 65.3; H, 5.2%). IR spectrum: 3045, 2980, 2960, 1585, 1570, 1545, 1480, 1450, 1435, 1400, 1380, 1335, 1310, 1280, 1260, 1185, 1160, 1115, 1100, 1070, 1055, 1025, 1000, 970, 935, 840, 815, 800, 745, 725, 710, 700, 655, 580, 560, 550, 530, 515, 485, 450, 345 and 330 cm⁻¹. Mass spectrum (FAB): *m/z* 717 {calc. for [⁵⁸Ni(tdpme)Cl]⁺, 717} and 682 {calc. for [⁵⁸Ni(tdpme)]⁺, 682}, with correct isotopic distributions. ³¹P-^{{1}H} NMR (CDCl₃, 293 K, 36.23 MHz): δ 29.21 (s, free PPh₂, 1P) and 25.98 (s, coordinated PPh₂, 2P).

[Ni([9]aneS₃)(dppm)][PF₆]₂. The complex [Ni(dppm)Cl₂] (0.172 g, 3.4 × 10⁻⁴ mol) was treated with [9]aneS₃ (0.030 g, 1.7 × 10⁻⁴ mol) in refluxing MeOH (10 cm³) for 1 h, yielding a dark red solution. Addition of NH₄PF₆ (0.054 g, 3.4 × 10⁻⁴ mol) and further refluxing for 30 min afforded a green precipitate, which was collected and recrystallised from MeCN-Et₂O. Yield 0.035 g, 23%. Alternatively, [Ni(dppm)Cl₂] (0.172 g, 3.4 × 10⁻⁴ mol), [9]aneS₃ (0.030 g, 1.7 × 10⁻⁴ mol) and TiPF₆ (0.112 g, 3.4 × 10⁻⁴ mol) were stirred in MeNO₂ (6 cm³) for 30 min, giving a dark red solution and a fine white precipitate. The solution was filtered and the product crystallised from the filtrate by addition of Et₂O. Yield 0.030 g, 20% (Found: C, 41.0; H, 3.8. Calc. for C₃₁H₃₄F₁₂NiP₄S₃: C, 40.8; H, 3.8%). IR spectrum: 3060, 3000, 2970, 2910, 1585, 1570, 1480, 1440, 1410, 1375, 1360, 1335, 1310, 1285, 1260, 1185, 1165, 1100, 1070, 1025, 1000, 940, 840, 750, 720, 705, 690, 660, 615, 555, 540, 500, 480, 455, 420 and 385 cm⁻¹. Electronic spectrum (MeCN): λ_{\max} 563 (ϵ_{\max} 124), 418 (1920), 317 (14 520) and 268 nm (20 180 dm³ mol⁻¹ cm⁻¹). Mass spectrum (FAB): m/z 805 {calc. for [⁵⁸Ni([9]aneS₃ - H)(dppm)(PF₆)⁺, 766}, 622 {calc. for [⁵⁸Ni([9]aneS₃)(dppm)⁺, 622} and 442 {calc. for [⁵⁸Ni(dppm)⁺, 442], with correct isotopic distributions. NMR (CD₃CN, 293 K): ¹H (200.13 MHz), δ 3.42–2.95 (m, [9]aneS₃ SCH₂, 12 H), 2.19 (d, ²J_{P-H} = 14.6 Hz, dcpe PCH₂, 4 H) and 2.12–1.07 [m, P(C₆H₁₁)₂, 44 H]; ¹³C (DEPT, 50.32 MHz), δ 36.98 [CH of (C₆H₁₁)₂], 36.25 (s, [9]aneS₃ SCH₂), 28.51, 27.41, 25.91, 25.60, 24.70 [s, CH₂ of (C₆H₁₁)₂] and 21.88 (apparent t, J = 20.1 Hz, dcpe PCH₂); ³¹P-{¹H} (36.23 MHz), δ 89.65 (s).

[Ni([9]aneS₃)(dppe)][PF₆]₂. Method as for [Ni([9]aneS₃)(dppm)][PF₆]₂, using [Ni(dppe)Cl₂] (0.088 g, 1.7 × 10⁻⁴ mol). The product was a dark green crystalline solid. Yield 0.13 g, 86% (Found: C, 41.4; H, 3.9. Calc. for C₃₂H₃₆F₁₂NiP₄S₃: C, 41.5; H, 3.9%). IR spectrum: 3040, 2980, 2940, 1580, 1570, 1480, 1435, 1410, 1380, 1340, 1305, 1290, 1235, 1180, 1160, 1100, 1060, 995, 945, 905, 875, 840, 810, 755, 725, 715, 705, 690, 660, 615, 560, 510, 485, 460, 450, 430, 385 and 365 cm⁻¹. Electronic spectrum (MeCN): λ_{\max} 560 (ϵ_{\max} 110), 427 (1765), 316 (16 970) and 256 nm (23 585 dm³ mol⁻¹ cm⁻¹). Mass spectrum (FAB): m/z 781 {calc. for [⁵⁸Ni([9]aneS₃)(dppe)(PF₆)⁺, 781}, 635 {calc. for [⁵⁸Ni([9]aneS₃ - H)(dppe)⁺, 635} and 455 {calc. for [⁵⁸Ni(dppe - H)⁺, 455], with correct isotopic distributions. NMR (CD₃NO₂, 293 K): ¹H (200.13 MHz), δ 7.88–7.63 (m, dppe PPh₂, 20 H), 3.22 (d, ²J_{P-H} = 18.8 Hz, dppe PCH₂, 4 H) and 2.96–2.38 (m, [9]aneS₃ SCH₂, 12 H); ¹³C (DEPT, 50.32 MHz), δ 132.52 (br), 131.61 (d, ³J_{P-C} = 4.4), 129.08 (d, ²J_{P-C} = 5.2, dppe PPh₂), 35.16 (s, [9]aneS₃ SCH₂) and 28.71 (apparent triplet, J = 23.8 Hz, dppe, PCH₂); ³¹P-{¹H} (36.23 MHz), δ 67.58 (s).

[Ni([9]aneS₃)(dppv)][PF₆]₂. Method as for [Ni([9]aneS₃)(dppm)][PF₆]₂, using [Ni(dppv)Cl₂] (0.088 g, 1.7 × 10⁻⁴ mol). The complex was a dark green crystalline solid. Yield 0.13 g, 82% (Found: C, 41.3; H, 3.7. Calc. for C₃₂H₃₄F₁₂NiP₄S₃: C, 41.5; H, 3.7%). IR spectrum: 3050, 3020, 2960, 1580, 1570, 1480, 1440, 1410, 1375, 1340, 1310, 1270, 1250, 1190, 1165, 1100, 1070, 1025, 1000, 985, 940, 840, 760, 735, 700, 620, 555, 525, 480, 455, 410 and 370 cm⁻¹. Electronic spectrum (MeCN): λ_{\max} 580 (ϵ_{\max} 65), 423 (1795), 320 (14 630) and 250 nm (28 650 dm³ mol⁻¹ cm⁻¹). Mass spectrum (FAB): m/z {calc. for [⁵⁸Ni([9]aneS₃)(dppv)(PF₆)⁺, 779}, 634 {calc. for [⁵⁸Ni([9]aneS₃)(dppv)⁺, 634} and 454 {calc. for [⁵⁸Ni(dppv)⁺, 454], with correct isotopic distributions. NMR (CD₃CN, 293 K): ¹H (200.13 MHz), δ 7.86–7.40 (m, dppv, PPh₂, 20 H), 2.90–2.28 (m, [9]aneS₃ SCH₂, 12 H) and 2.08 (s, dppv PCH, 2 H); ¹³C-{¹H} (50.32 MHz), δ 146.35 (apparent t, J = 37.5, dppv CH), 133.40, 132.40, 129.81 (br), 126.18 (apparent t, J = 26.4 Hz, dppv PPh₂) and 36.12 (s, [9]aneS₃ SCH₂); ³¹P-{¹H} (36.23 MHz), δ 75.52 (s).

[Ni([9]aneS₃)(dcpe)][PF₆]₂. Method as for [Ni([9]aneS₃)(dppm)][PF₆]₂, using [Ni(dcpe)Cl₂] (0.092 g, 1.7 × 10⁻⁴ mol). The product was a dark red crystalline solid. Yield 0.14 g, 88% (Found: C, 41.1; H, 6.4; N, 1.5. Calc. for C₃₂H₆₀F₁₂NiP₄S₃·CH₃CN: C, 41.1; H, 6.4; N, 1.4%). IR spectrum: 2990, 2920,

2840, 2800, 1440, 1405, 1370, 1345, 1325, 1300, 1290, 1270, 1245, 1205, 1175, 1150, 1115, 1090, 1070, 1040, 1005, 940, 910, 840, 750, 735, 670, 650, 620, 555, 530, 515, 480, 455, 390 and 360 cm⁻¹. Electronic spectrum (MeCN): λ_{\max} 570 (ϵ_{\max} 200), 448 (775), 325 (6730), 293 (12 670) and 245 (13 190 dm³ mol⁻¹ cm⁻¹). Mass spectrum (FAB): m/z 805 {calc. for [⁵⁸Ni([9]aneS₃)(dcpe)(PF₆)⁺, 805}, 660 {calc. for [⁵⁸Ni([9]aneS₃)(dcpe)⁺, 660} and 480 {calc. for [⁵⁸Ni(dcpe)⁺, 480], with correct isotopic distributions. NMR (CD₃CN, 293 K): ¹H (200.13 MHz), δ 3.42–2.95 (m, [9]aneS₃ SCH₂, 12 H), 2.19 (d, ²J_{P-H} = 14.6 Hz, dcpe PCH₂, 4 H) and 2.12–1.07 [m, P(C₆H₁₁)₂, 44 H]; ¹³C (DEPT, 50.32 MHz), δ 36.98 [CH of (C₆H₁₁)₂], 36.25 (s, [9]aneS₃ SCH₂), 28.51, 27.41, 25.91, 25.60, 24.70 [s, CH₂ of (C₆H₁₁)₂] and 21.88 (apparent t, J = 20.1 Hz, dcpe PCH₂); ³¹P-{¹H} (36.23 MHz), δ 89.65 (s).

[Ni([9]aneS₃)(dmpe)][PF₆]₂. Method as for [Ni([9]aneS₃)(dppm)][PF₆]₂, using [Ni(dmpe)Cl₂] (0.047 g, 1.7 × 10⁻⁴ mol). The product was a dark red microcrystalline solid. Yield 0.080 g, 71% (Found: C, 21.0; H, 4.2. Calc. for C₁₂H₂₈F₁₂NiP₄S₃: C, 21.1; H, 4.2%). IR spectrum: 3000, 2945, 2920, 1450, 1420, 1295, 1275, 1240, 1180, 1085, 1010, 995, 950, 920, 905, 840, 745, 720, 690, 665, 650, 620, 555, 485, 470, 460, 440, 380 and 360 cm⁻¹. Electronic spectrum (MeCN): λ_{\max} 540 (ϵ_{\max} 166), 415 (662), 284 (13 150) and 249 nm (17 380 dm³ mol⁻¹ cm⁻¹). Mass spectrum (FAB): m/z 533 {calc. for [⁵⁸Ni([9]aneS₃)(dmpe)(PF₆)⁺, 533}, and 388 {calc. for [⁵⁸Ni([9]aneS₃)(dmpe)⁺, 388], with correct isotopic distributions. NMR (CD₃CN, 293 K): ¹H (200.13 MHz), δ 3.22–2.91 (m, [9]aneS₃ SCH₂, 12 H), 2.17 (br, dmpe PCH₂, 4 H) and 1.66 (m, dmpe PCH₃, 12 H); ¹³C (DEPT, 50.32 MHz), δ 35.69 (s, [9]aneS₃ SCH₂), 26.89 (apparent t, J = 25.9, dmpe PCH₂), 13.58 (apparent t, J = 14.7) and 13.49 (apparent t, J = 14.4 Hz, dmpe PCH₃); ³¹P-{¹H} (36.23 MHz), δ 58.02 (s).

[Ni([9]aneS₃)(dppp)][PF₆]₂. Method as for [Ni([9]aneS₃)(dppm)][PF₆]₂, using [Ni(dppp)Cl₂] (0.090 g, 1.7 × 10⁻⁴ mol). The product was an olive green crystalline solid. Yield 0.13 g, 80% (Found: C, 43.3; H, 4.3; N, 2.1. Calc. for C₃₃H₃₈F₁₂NiP₄S₃·1.5CH₃CN: C, 43.1; H, 4.3; N, 2.1%). IR spectrum: 3070, 3050, 2990, 2950, 2920, 2850, 1580, 1570, 1480, 1445, 1435, 1415, 1395, 1370, 1340, 1320, 1300, 1270, 1250, 1190, 1150, 1130, 1090, 1070, 1050, 1025, 995, 975, 930, 915, 920, 840, 780, 755, 745, 700, 665, 615, 555, 530, 510, 490, 480, 425 and 375 cm⁻¹. Electronic spectrum (MeCN): λ_{\max} 600 (ϵ_{\max} 133), 452 (1365), 335 (15 860) and 260 nm (11 990 dm³ mol⁻¹ cm⁻¹). Mass spectrum (FAB): m/z 794 {calc. for [⁵⁸Ni([9]aneS₃ - H)(dppp)(PF₆)⁺, 794}, 650 {calc. for [⁵⁸Ni([9]aneS₃)(dppp)⁺, 650} and 470 {calc. for [⁵⁸Ni(dppp)⁺, 470], with correct isotopic distributions. NMR (CD₃CN, 293 K): ¹H (200.13 MHz), δ 7.69–7.50 (m, dppp PPh₂, 20 H), 2.81 (dt, ²J_{P-H} = 9.7, ³J_{H-H} = 5.8 Hz, dppp PCH₂CH₂, 4 H), 2.75–2.32 (m, [9]aneS₃ SCH₂, 12 H) and 2.19 (br, dppp PCH₂CH₂, 2 H); ¹³C (DEPT, 50.32 MHz): δ 132.51, 132.29, 129.17 (br, dppp PPh₂), 36.39 (s, [9]aneS₃ SCH₂), 23.27 (apparent t, J = 18.5 Hz, PCH₂CH₂) and 16.39 (s, PCH₂CH₂); ³¹P-{¹H} (36.23 MHz), δ 2.29 (s).

[Ni([9]aneS₃)(tdpme)][PF₆]₂. Method as for [Ni([9]aneS₃)(dppm)][PF₆]₂, using [Ni(tdpme)Cl₂] (0.128 g, 1.7 × 10⁻⁴ mol). The complex was an olive green microcrystalline solid. Yield 0.15 g, 78% (Found: C, 48.6; H, 4.5. Calc. for C₄₇H₅₁F₁₂NiP₅S₃: C, 48.9; H, 4.4%). IR spectrum: 3060, 3000, 2960, 2940, 2910, 1585, 1570, 1480, 1460, 1445, 1435, 1410, 1385, 1320, 1300, 1270, 1245, 1200, 1190, 1170, 1160, 1115, 1090, 1065, 1040, 1000, 960, 940, 840, 745, 715, 700, 615, 555, 535, 510, 500, 485, 455, 440 and 410 cm⁻¹. Electronic spectrum (MeCN): λ_{\max} 593 (ϵ_{\max} 46.1), 445 (1280), 333 (11 300) and 250 nm (19 900 dm³ mol⁻¹ cm⁻¹). Mass spectrum (FAB): m/z 1007 {calc. for [⁵⁸Ni([9]aneS₃)(tdpme)(PF₆)⁺, 1007}, 861 {calc. for [⁵⁸Ni([9]aneS₃ - H)(tdpme)⁺, 861} and 682 {calc. for [⁵⁸Ni(tdpme)⁺, 682], with correct isotopic distributions. NMR (CD₃CN, 293 K): ¹H (200.13 MHz), δ 7.87–7.06 (m, tdpme PPh₂, 30 H), 2.74–2.07 (m, [9]aneS₃ SCH₂ and tdpme PCH₂, 18 H) and 0.42 (s, tdpme CCH₃, 3 H); ¹³C (DEPT, 50.32

Table 8 Experimental data for single-crystal structure determinations of $[\text{Ni}([9]\text{aneS}_3)(\text{L-L})][\text{PF}_6]_2$ ^a

L-L	dppm	dcpe	tdpme
Molecular formula	$\text{C}_{31}\text{H}_{34}\text{F}_{12}\text{NiP}_4\text{S}_3$	$\text{C}_{32}\text{H}_{60}\text{F}_{12}\text{NiP}_4\text{S}_3 \cdot 1.25\text{CH}_3\text{CN}$	$\text{C}_{47}\text{H}_{51}\text{F}_{12}\text{NiP}_5\text{S}_3$
M_r	913.25	1002.79	1153.5
Crystal system	Triclinic	Triclinic	Monoclinic
Space group	$P\bar{1}$	$P\bar{1}$	Cc
$a/\text{\AA}$	10.9748(25)	12.432(8)	10.7597(16)
$b/\text{\AA}$	13.9702(20)	13.382(4)	37.399(5)
$c/\text{\AA}$	15.7688(24)	15.070(6)	13.104(3)
$\alpha/^\circ$	80.071(7)	86.83(2)	
$\beta/^\circ$	70.817(8)	70.47(2)	103.746(11)
$\gamma/^\circ$	76.441(8)	77.28(2)	
$U/\text{\AA}^3$	2208	2305	5139
Z	2	2	4
$D_c/\text{g cm}^{-3}$	1.374	1.445	1.491
Crystal appearance	Dark red tablet	Red platelet	Brown needle
Crystal dimensions/mm	0.47 × 0.39 × 0.19	0.58 × 0.51 × 0.12	0.65 × 0.06 × 0.05
$\mu(\text{Mo-K}\alpha)/\text{mm}^{-1}$	0.789	0.763	0.724
$F(000)$	928	1047	2368
Scan width	Learnt profile method	$0.99 + 0.347 \tan\theta (\omega/^\circ)$	Learnt profile method
Index ranges h, k, l	-10 to 11, -14 to 15, 0-16	-12 to 13, -14 to 14, 0-16	-11 to 11, 0-40, 0-14
Data measured	5762	6021	3962
Data used [$F > n(F)$] (N_o)	4405	3667	2204
n	4	4	6
Weighting scheme w^{-1}	$\sigma^2(F) + 0.00041F^2$	$\sigma^2(F) + 0.00035F^2$	$\sigma^2(F) + 0.00038F^2$
Final R, R'	0.0689, 0.0970	0.0491, 0.0627	0.0567, 0.0663
Final S^b	1.191	1.053	1.164
No. of parameters refined (N_p)	434	508	352
Maximum, minimum residues in final ΔF synthesis/e \AA^{-3}	0.86, -0.48	0.51, -0.29	0.60, -0.27

^a Details in common: Stoö Stadi-4 four-circle diffractometer, $T = 298 \text{ K}$, $\omega-2\theta$ scan mode, graphite monochromated Mo-K α radiation ($\lambda = 0.71073 \text{ \AA}$), $2\theta_{\max} = 45^\circ$, no absorption correction. ^b S (goodness of fit) = $[\sum w(|F_o| - |F_c|)^2 / (N_o - N_p)]^{1/2}$.

Table 9 Atomic coordinates with e.s.d.s in parentheses for $[\text{Ni}([9]\text{aneS}_3)(\text{dppm})][\text{PF}_6]_2$

Atom	x	y	z	Atom	x	y	z
Ni	0.433 02(8)	0.232 89(6)	0.162 12(5)	C(42)	0.367 5(5)	0.342 2(4)	0.467 1(3)
S(1)	0.477 78(18)	0.101 75(13)	0.069 44(13)	C(43)	0.275 3(5)	0.316 8(4)	0.548 2(3)
C(2)	0.649 5(9)	0.055 3(9)	0.061 5(8)	C(44)	0.199 4(5)	0.248 0(4)	0.551 9(3)
C(2')	0.625 3(13)	0.031 1(8)	0.096 1(13)	C(45)	0.215 7(5)	0.204 5(4)	0.474 7(3)
C(3)	0.678 6(11)	0.061 4(7)	0.146 8(8)	C(46)	0.308 0(5)	0.229 9(4)	0.393 6(3)
C(3')	0.713 6(9)	0.097 9(13)	0.098 9(13)	C(51)	0.473 1(6)	0.013 1(4)	0.369 5(4)
S(4)	0.631 32(18)	0.187 66(19)	0.180 25(15)	C(52)	0.528 6(6)	-0.087 0(4)	0.381 8(4)
C(5)	0.734 4(8)	0.252 2(10)	0.082 9(9)	C(53)	0.490 4(6)	-0.157 2(4)	0.347 8(4)
C(5')	0.706 8(16)	0.292 8(13)	0.114 9(12)	C(54)	0.396 8(6)	-0.127 4(4)	0.301 6(4)
C(6)	0.659 0(10)	0.349 9(8)	0.055 4(9)	C(55)	0.341 4(6)	-0.027 4(4)	0.289 4(4)
C(6')	0.680 6(11)	0.316 9(17)	0.025 1(10)	C(56)	0.379 5(6)	0.042 9(4)	0.323 3(4)
S(7)	0.504 15(21)	0.337 58(15)	0.040 99(14)	P(10)	0.050 61(21)	0.914 93(16)	0.187 50(15)
C(8)	0.568 4(12)	0.258 2(6)	-0.050 8(5)	F(11)	1.186 1(5)	-0.046 2(5)	0.149 8(4)
C(8')	0.493(3)	0.273 2(7)	-0.047 5(8)	F(12)	1.026 1(8)	-0.038 1(7)	0.096 6(5)
C(9)	0.493 0(14)	0.178 0(6)	-0.037 9(6)	F(13)	0.916 2(6)	-0.123 7(5)	0.221 1(5)
C(9')	0.552 7(23)	0.165 8(7)	-0.039 2(7)	F(14)	1.074 6(11)	-0.135 8(8)	0.274 5(6)
P(1)	0.224 82(16)	0.290 26(12)	0.180 92(11)	F(15)	1.115 7(7)	-0.181 1(5)	0.136 8(6)
C(21)	0.248 4(3)	0.468 9(3)	0.221 6(4)	F(16)	0.985 6(10)	0.012 0(6)	0.223 6(8)
C(22)	0.199 3(3)	0.565 1(3)	0.246 0(4)	P(20)	0.597 49(25)	0.544 58(21)	0.252 41(19)
C(23)	0.064 9(3)	0.603 8(3)	0.265 7(4)	F(21)	0.668 6(11)	0.635 3(9)	0.240 8(11)
C(24)	-0.020 4(3)	0.546 2(3)	0.261 1(4)	F(22)	0.462 4(8)	0.625 4(8)	0.270 4(8)
C(25)	0.028 7(3)	0.450 1(3)	0.236 7(4)	F(23)	0.526 0(14)	0.459 5(11)	0.266 3(10)
C(26)	0.163 0(3)	0.411 4(3)	0.216 9(4)	F(24)	0.734 7(13)	0.473 0(10)	0.226 5(14)
C(31)	0.142 7(5)	0.370 21(25)	0.031 6(3)	F(25)	0.594 9(19)	0.531 0(12)	0.352 1(8)
C(32)	0.100 1(5)	0.366 74(25)	-0.041 8(3)	F(26)	0.610 0(14)	0.560 9(8)	0.148 7(7)
C(33)	0.073 6(5)	0.278 63(25)	-0.055 3(3)	F(21')	0.533(3)	0.530 0(20)	0.184 4(19)
C(34)	0.089 5(5)	0.194 00(25)	0.004 5(3)	F(22')	0.731(4)	0.499(3)	0.183 7(22)
C(35)	0.132 1(5)	0.197 48(25)	0.077 9(3)	F(23')	0.467(3)	0.561(3)	0.315 1(22)
C(36)	0.158 7(5)	0.285 58(25)	0.091 5(3)	F(24')	0.670(5)	0.573(4)	0.296(4)
C(10)	0.168 5(6)	0.200 2(5)	0.275 0(4)	F(25')	0.604(5)	0.433(4)	0.274(3)
P(2)	0.327 35(17)	0.172 58(13)	0.296 27(11)	F(26')	0.624(3)	0.646 7(22)	0.198 4(20)
C(41)	0.383 8(5)	0.298 8(4)	0.389 8(3)	O(1S)	0.118 5(23)	0.756 8(17)	0.572 2(16)

MHz), δ 133.25–128.07 (m, tdpme PPh_2), 36.53 (s, [9]aneS₃ SCH₂), 35.70 (apparent t, $J = 15.4$, tdpme co-ordinated PCH₂), 35.20 (apparent t, $J = 17.8$ Hz, tdpme free PCH₂)

and 10.3 (s, tdpme CCH₃); $^{31}\text{P}-\{{}^1\text{H}\}$ (36.23 MHz), δ 9.02 (s, tdpme co-ordinated PPh_2 , 2P) and 7.54 (s, tdpme free PPh_2 , 1P). $[{}^6\text{Ni}([9]\text{aneS}_3)(\text{tdpme})][\text{PF}_6]_2$. 62% Labelled ${}^6\text{Ni}(\text{NO}_3)_2$.

Table 10 Atomic coordinates with e.s.d.s in parentheses for $[\text{Ni}([9]\text{aneS}_3)(\text{dcpe})][\text{PF}_6]_2 \cdot 1.25\text{MeCN}$

Atom	<i>x</i>	<i>y</i>	<i>z</i>	Atom	<i>x</i>	<i>y</i>	<i>z</i>
Ni	0.105 37(7)	0.184 19(6)	0.222 19(5)	C(44)	0.320 5(6)	0.291 3(6)	0.461 3(5)
S(1)	-0.000 21(15)	0.110 23(13)	0.371 87(12)	C(45)	0.304 7(5)	0.258 8(5)	0.371 6(5)
C(2)	0.125 5(6)	0.044 4(6)	0.405 9(5)	C(46)	0.204 6(5)	0.336 3(5)	0.350 4(4)
C(3)	0.231 5(6)	-0.003 9(5)	0.325 7(5)	C(51)	0.330 6(6)	0.284 8(6)	0.048 1(5)
S(4)	0.270 82(14)	0.079 68(12)	0.225 76(12)	C(52)	0.455 0(6)	0.260 6(6)	-0.021 8(5)
C(5)	0.304 2(6)	-0.007 8(5)	0.127 2(5)	C(53)	0.520 1(7)	0.343 1(7)	-0.019 5(6)
C(6)	0.198 4(6)	-0.048 0(5)	0.128 1(5)	C(54)	0.518 5(6)	0.360 3(6)	0.079 6(6)
S(7)	0.072 25(16)	0.059 37(13)	0.144 68(12)	C(55)	0.395 0(6)	0.386 2(5)	0.150 1(5)
C(8)	-0.042 7(6)	0.010 0(6)	0.232 2(5)	C(56)	0.331 6(5)	0.300 0(5)	0.147 6(4)
C(9)	-0.036 0(6)	-0.000 1(5)	0.330 8(5)	P(10)	0.235 89(19)	0.686 07(15)	0.328 79(14)
P(1)	-0.025 00(14)	0.303 47(12)	0.180 60(12)	F(11)	0.353 7(5)	0.607 4(4)	0.316 1(5)
C(11)	0.030 6(5)	0.421 5(4)	0.153 2(5)	F(12)	0.294 6(6)	0.749 8(4)	0.242 1(4)
C(12)	0.099 2(5)	0.436 2(4)	0.217 3(5)	F(13)	0.118 9(5)	0.767 7(4)	0.339 7(5)
C(21)	-0.182 0(6)	0.391 1(6)	0.357 9(5)	F(14)	0.176 8(5)	0.628 3(5)	0.418 2(4)
C(22)	-0.307 6(6)	0.435 7(6)	0.415 8(5)	F(15)	0.268 4(6)	0.757 2(4)	0.390 4(4)
C(23)	-0.381 7(6)	0.354 3(7)	0.433 2(5)	F(16)	0.204 4(7)	0.617 1(4)	0.265 8(5)
C(24)	-0.373 6(6)	0.307 9(7)	0.341 8(6)	P(20)	0.633 38(17)	0.015 71(17)	0.174 35(16)
C(25)	-0.246 5(6)	0.262 8(6)	0.284 2(5)	F(21)	0.573 9(7)	0.114 4(5)	0.234 1(6)
C(26)	-0.174 8(5)	0.344 9(5)	0.265 2(4)	F(22)	0.742 3(5)	0.060 2(6)	0.117 1(5)
C(31)	-0.138 4(6)	0.354 7(6)	0.042 8(5)	F(23)	0.688 3(6)	-0.080 3(5)	0.110 0(5)
C(32)	-0.158 2(6)	0.317 8(6)	-0.043 7(5)	F(24)	0.526 6(5)	-0.031 2(5)	0.233 4(5)
C(33)	-0.045 6(6)	0.288 4(6)	-0.125 0(5)	F(25)	0.566 5(5)	0.062 1(5)	0.104 1(4)
C(34)	0.044 5(6)	0.209 1(5)	-0.095 7(5)	F(26)	0.698 5(5)	-0.034 0(6)	0.243 3(4)
C(35)	0.065 8(5)	0.248 9(5)	-0.011 8(4)	C(1S)	0.582 1(8)	0.723 1(8)	0.290 0(7)
C(36)	-0.049 0(5)	0.271 9(5)	0.071 8(4)	C(2S)	0.677 0(9)	0.652 1(8)	0.226 8(8)
P(2)	0.186 04(14)	0.313 02(12)	0.237 20(12)	N(1S)	0.751 8(9)	0.598 8(8)	0.179 1(8)
C(41)	0.091 7(5)	0.347 4(5)	0.433 6(4)	C(3S)	0.447 2(16)	0.994 4(17)	0.505 7(15)
C(42)	0.109 4(6)	0.378 1(6)	0.522 7(5)	C(4S)	0.649(3)	0.005 4(25)	0.479 3(20)
C(43)	0.208 1(6)	0.303 4(7)	0.543 5(5)				

Table 11 Atomic coordinates with e.s.d.s in parentheses for $[\text{Ni}([9]\text{aneS}_3)(\text{tdpme})][\text{PF}_6]_2$

Atom	<i>x</i>	<i>y</i>	<i>z</i>	Atom	<i>x</i>	<i>y</i>	<i>z</i>
Ni	0.000 0	-0.081 72(5)	0.000 0	C(63)	-0.006 9(11)	-0.237 02(25)	-0.448 2(8)
S(1)	-0.027 6(5)	-0.047 77(12)	0.153 7(4)	C(64)	-0.064 1(11)	-0.203 79(25)	-0.444 1(8)
C(2)	-0.002 2(21)	-0.001 9(5)	0.114 8(15)	C(65)	-0.131 2(11)	-0.197 03(25)	-0.367 3(8)
C(3)	-0.018 7(19)	0.005 3(4)	0.002 6(14)	C(66)	-0.140 9(11)	-0.223 51(25)	-0.294 6(8)
S(4)	0.038 0(4)	-0.029 61(11)	-0.075 3(3)	C(71)	-0.455 2(11)	-0.256 3(3)	-0.229 3(7)
C(5)	0.207 7(17)	-0.025 2(5)	-0.043 4(15)	C(72)	-0.580 9(11)	-0.265 0(3)	-0.278 3(7)
C(6)	0.279 6(17)	-0.059 0(5)	-0.012 0(15)	C(73)	-0.645 1(11)	-0.245 9(3)	-0.366 7(7)
S(7)	0.209 1(4)	-0.086 33(12)	0.074 2(3)	C(74)	-0.583 6(11)	-0.218 2(3)	-0.406 1(7)
C(8)	0.237 9(18)	-0.057 7(6)	0.192 7(15)	C(75)	-0.457 9(11)	-0.209 5(3)	-0.357 1(7)
C(9)	0.122 5(16)	-0.056 9(5)	0.240 5(12)	C(76)	-0.393 7(11)	-0.228 5(3)	-0.268 7(7)
P(1)	-0.012 4(4)	-0.139 55(11)	0.035 9(3)	C(11)	-0.390 3(15)	-0.175 6(4)	-0.067 2(13)
C(21)	0.096 4(10)	-0.203 5(3)	-0.003 1(7)	C(12)	-0.272 6(14)	-0.115 2(4)	-0.082 3(11)
C(22)	0.164 7(10)	-0.225 7(3)	-0.055 4(7)	C(13)	-0.163 5(15)	-0.162 7(4)	0.018 6(11)
C(23)	0.219 3(10)	-0.211 7(3)	-0.133 2(7)	C(14)	-0.304 8(13)	-0.115 2(3)	-0.087 7(11)
C(24)	0.205 5(10)	-0.175 4(3)	-0.158 7(7)	C(15)	-0.232 7(16)	-0.169 1(4)	-0.179 7(11)
C(25)	0.137 1(10)	-0.153 2(3)	-0.106 3(7)	P(10)	0.084 5(5)	-0.375 96(17)	-0.263 6(4)
C(26)	0.082 5(10)	-0.167 2(3)	-0.028 5(7)	F(11A)	-0.535(3)	0.141 4(7)	-0.340 3(22)
C(31)	0.181 4(8)	-0.155 9(3)	0.214 0(7)	F(12A)	-0.461(4)	0.111 0(11)	-0.381(3)
C(32)	0.233 8(8)	-0.157 5(3)	0.322 0(7)	F(13A)	-0.307(5)	0.124 6(13)	-0.179(3)
C(33)	0.159 1(8)	-0.149 2(3)	0.392 2(7)	F(14A)	-0.401(3)	0.148 6(7)	-0.162 8(20)
C(34)	0.031 9(8)	-0.139 2(3)	0.354 3(7)	F(15A)	-0.333 5(23)	0.152 0(7)	0.322 1(20)
C(35)	-0.020 5(8)	-0.137 6(3)	0.246 3(7)	F(16A)	-0.500(3)	0.094 6(8)	-0.231(3)
C(36)	0.054 3(8)	-0.145 9(3)	0.176 2(7)	F(11B)	-0.479(3)	0.085 6(10)	-0.327(3)
P(2)	-0.190 3(4)	-0.083 30(10)	-0.110 2(3)	F(12B)	-0.354(4)	0.111 5(9)	-0.351(3)
C(41)	-0.294 2(11)	-0.017 0(3)	-0.183 5(7)	F(13B)	-0.333(3)	0.161 8(9)	-0.270(3)
C(42)	-0.361 4(11)	0.014 4(3)	-0.176 3(7)	F(14B)	-0.476(3)	0.105 8(8)	-0.181 2(23)
C(43)	-0.411 5(11)	0.020 4(3)	-0.089 0(7)	F(15B)	-0.523(3)	0.150 7(7)	-0.279 0(22)
C(44)	-0.394 5(11)	-0.005 0(3)	-0.008 9(7)	F(16B)	-0.293 4(19)	0.099 3(6)	-0.212 8(15)
C(45)	-0.327 3(11)	-0.036 4(3)	-0.016 1(7)	P(20)	-0.680 4(5)	-0.069 37(16)	-0.331 6(5)
C(46)	-0.277 2(11)	-0.042 4(3)	-0.103 3(7)	F(21)	-0.572 2(12)	-0.072 7(4)	-0.226 5(10)
C(51)	-0.069 1(7)	-0.090 0(3)	-0.276 9(6)	F(22)	-0.787 6(11)	-0.064 2(4)	-0.436 0(9)
C(52)	-0.068 6(7)	-0.094 7(3)	-0.382 4(6)	F(23A)	-0.587 6(23)	-0.046 9(8)	-0.381 3(18)
C(53)	-0.183 6(7)	-0.097 1(3)	-0.458 1(6)	F(24A)	-0.726(3)	-0.032 2(8)	-0.288 6(19)
C(54)	-0.299 0(7)	-0.094 7(3)	-0.428 2(6)	F(25A)	-0.763 4(20)	-0.089 9(6)	-0.269 0(16)
C(55)	-0.299 5(7)	-0.090 0(3)	-0.322 7(6)	F(26A)	-0.630 1(25)	-0.102 9(7)	-0.367 9(19)
C(56)	-0.184 5(7)	-0.087 6(3)	-0.247 1(6)	F(23B)	-0.590(4)	-0.078 7(13)	-0.412(3)
P(3)	-0.227 8(5)	-0.218 62(11)	-0.192 5(4)	F(24B)	-0.632(4)	-0.028 9(11)	-0.347(3)
C(61)	-0.083 6(11)	-0.256 75(25)	-0.298 8(8)	F(25B)	-0.779(3)	-0.055 0(9)	-0.275 8(21)
C(62)	-0.016 6(11)	-0.263 50(25)	-0.375 6(8)	F(26B)	-0.742(4)	-0.108 9(10)	-0.334(3)

$6\text{H}_2\text{O}$ (0.027 g , $9.4 \times 10^{-5}\text{ mol}$) was treated with tdpme (0.058 g , $9.4 \times 10^{-5}\text{ mol}$) in refluxing MeOH (15 cm^3) for 30 min , yielding an olive green solution. $1,4,7\text{-Trithiacyclononane}$ (0.017 g , $9.4 \times 10^{-5}\text{ mol}$) was then added, and the mixture refluxed for 30 min . Addition of NH_4PF_6 (0.31 g , $1.9 \times 10^{-4}\text{ mol}$) quickly gave a green precipitate, which was collected and recrystallised from MeCN–Et₂O. Yield 0.060 g , 55% (Found: C, 48.9% ; H, 4.5% . Calc. for $\text{C}_{47}\text{H}_{51}\text{F}_{12}{^{61}\text{NiS}_3\text{P}_5}$: C, 48.9% ; H, 4.5%).

Single-crystal Structure Determinations.—Single crystals of X-ray quality of $[\text{Ni}([9]\text{aneS}_3)(\text{dppm})][\text{PF}_6]_2$, $[\text{Ni}([9]\text{aneS}_3)(\text{dcpe})][\text{PF}_6]_2$ · 1.25MeCN and $[\text{Ni}([9]\text{aneS}_3)(\text{tdpme})][\text{PF}_6]_2$ were obtained by diffusion of Et₂O vapour into MeCN solutions of the complexes: a suitable crystal was mounted on a glass fibre, or (for L–L = dcpe) sealed into a Lindemann tube to prevent solvent loss. Details of the crystal data, data collection and processing and structure analysis and refinement are given in Table 8. All three structures were solved using a Patterson synthesis and developed by iterative cycles of least-squares refinement and Fourier difference syntheses.³⁵ Hydrogen atoms were included in fixed, calculated positions and (for L–L = dppm or tdpme) phenyl rings were refined as rigid hexagonal groups.³⁵ Tables 1–3 give bond lengths and angles while atomic coordinates appear in Tables 9–11. Illustrations were obtained using ORTEP,³⁶ and molecular geometry calculations utilised CALC.³⁷ Scattering factor data were inlaid or taken from ref. 38. Details of individual structure refinements are given below.

$[\text{Ni}([9]\text{aneS}_3)(\text{dppm})][\text{PF}_6]_2$. During refinement, the [9]aneS₃ methylene groups were found to be disordered over two equally occupied orientations; this was successfully modelled using the constrained parameters S–C 1.83, C–C 1.52 Å, S–C–C 109°. One PF_6^- anion was also found to be disordered, and was modelled over two distinct orientations with 70:30 occupancy ratio. Anisotropic thermal parameters were refined for all non-H atoms with site occupancy factor >0.5.

$[\text{Ni}([9]\text{aneS}_3)(\text{dcpe})][\text{PF}_6]_2$ · 1.25MeCN . One quarter-occupied MeCN solvent molecule was found to be disordered about a crystallographic inversion centre at the centre of the C≡N bond. Anisotropic thermal parameters were refined for all wholly occupied non-H atoms.

$[\text{Ni}([9]\text{aneS}_3)(\text{tdpme})][\text{PF}_6]_2$. Both PF_6^- anions were found to be disordered: one over two discrete orientations and one by rotation about a F–P–F axis. Both were satisfactorily modelled using partial-site occupancies such that the total occupancy of F atoms for each anion equalled 6. Anisotropic thermal parameters were refined for Ni, S, P, wholly occupied F and non-aryl C atoms. The absolute structure was not determined.

Additional material available from the Cambridge Crystallographic Data Centre comprises H-atom coordinates, thermal parameters and remaining bond lengths and angles.

Acknowledgements

We thank the SERC and ICI Colours and Fine Chemicals for a CASE award (to M. A. H.), the SERC for support, the Royal Society of Edinburgh and Scottish Office Education Department for a Support Research Fellowship (to M. S.), and the Royal Society for support. We thank Dr. David Collison (University of Manchester) for helpful discussions.

References

- K. Nag and A. Chakravorty, *Coord. Chem. Rev.*, 1980, **33**, 87; A. G. Lappin and A. McAuley, *Adv. Inorg. Chem.*, 1988, **32**, 241.
- R. Cammack, *Adv. Inorg. Chem.*, 1988, **32**, 297 and refs. therein; L. R. Furenlid, M. W. Renner and J. Fajer, *J. Am. Chem. Soc.*, 1990, **112**, 8987.
- R. R. Gagné and D. M. Ingle, *J. Am. Chem. Soc.*, 1980, **102**, 1444; *Inorg. Chem.*, 1981, **20**, 420; J. Lewis and M. Schröder, *J. Chem. Soc., Dalton Trans.*, 1982, 1085; K. M. Kadish, M. M. Franzen, B. C. Han, C. Araullo-McAdams and D. Sazou, *J. Am. Chem. Soc.*, 1991, **113**, 512; P. Stavropoulos, M. C. Muetterties, M. Carrié and R. H. Holm, *J. Am. Chem. Soc.*, 1991, **113**, 8485.
- B. Fischer and R. Eisenberg, *J. Am. Chem. Soc.*, 1980, **102**, 7361; M. Beley, J. P. Collin, R. Ruppert and J.-P. Sauvage, *J. Chem. Soc., Chem. Commun.*, 1984, 1315; *J. Am. Chem. Soc.*, 1986, **108**, 7461; D. A. Gangi and R. R. Durand, *J. Chem. Soc., Chem. Commun.*, 1986, 697.
- P. Chmielewski, M. Grzeszczuk, L. Latos-Grazynski and J. Lisowski, *Inorg. Chem.*, 1989, **28**, 3546.
- C. Gosden, K. P. Healey and D. Pletcher, *J. Chem. Soc., Dalton Trans.*, 1978, 978; K. P. Healey and D. Pletcher, *J. Organomet. Chem.*, 1978, **161**, 109; C. Gosden and D. Pletcher, *J. Organomet. Chem.*, 1980, **186**, 401; J. Y. Becker, J. B. Kerr, D. Pletcher and R. Rosas, *J. Electroanal. Chem. Interfacial Chem.*, 1981, **117**, 87; C. Gosden, J. B. Kerr, D. Pletcher and R. Rosas, *J. Electroanal. Chem. Interfacial Chem.*, 1981, **117**, 101.
- A. Bakac and J. H. Espenson, *J. Am. Chem. Soc.*, 1986, **108**, 713; M. S. Ram, A. Bakac and J. H. Espenson, *Inorg. Chem.*, 1986, **25**, 3267.
- M. Schröder, *Pure Appl. Chem.*, 1988, **60**, 517; A. J. Blake and M. Schröder, *Adv. Inorg. Chem.*, 1990, **35**, 1; G. Reid and M. Schröder, *Chem. Soc. Rev.*, 1990, **19**, 239.
- M. A. Halcrow, Ph.D. Thesis, University of Edinburgh, 1991; A. J. Blake, R. O. Gould, M. A. Halcrow, A. J. Holder, T. I. Hyde and M. Schröder, *J. Chem. Soc., Dalton Trans.*, 1992, 3427.
- S. Chandrasekhar and A. McAuley, *Inorg. Chem.*, 1992, **31**, 480; K. Wieghardt, H.-J. Küppers and J. Weiss, *Inorg. Chem.*, 1985, **24**, 3067; W. N. Setzer, C. A. Ogle, G. S. Wilson and R. S. Glass, *Inorg. Chem.*, 1983, **22**, 266.
- H.-J. Küppers, K. Wieghardt, Y.-H. Tsay, C. Krüger, B. Nuber and J. Weiss, *Angew. Chem., Int. Ed. Engl.*, 1987, **26**, 575; P. J. Blower, J. A. Clarkson, S. C. Rawle, J.-A. R. Hartman, R. E. Wolf, R. Yagbasan, S. G. Bott and S. R. Cooper, *Inorg. Chem.*, 1989, **28**, 4040; A. J. Blake, R. O. Gould, A. J. Holder, T. I. Hyde and M. Schröder, *Polyhedron*, 1989, **8**, 513.
- A. J. Blake, R. O. Gould, J. A. Greig, A. J. Holder, T. I. Hyde and M. Schröder, *J. Chem. Soc., Chem. Commun.*, 1989, 876.
- A. J. Blake, J. A. Greig, A. J. Holder, T. I. Hyde, A. Taylor and M. Schröder, *Angew. Chem., Int. Ed. Engl.*, 1990, **29**, 197; A. J. Blake, R. O. Gould, C. Radek, G. Reid, A. Taylor and M. Schröder, *Proceedings of the 1st International Conference on the Chemistry of the Copper and Zinc Triads*, Edinburgh, Royal Society of Chemistry, 1993, pp. 95–102.
- G. Booth and J. Chatt, *J. Chem. Soc.*, 1965, 3238; G. R. Van Hecke and W. DeW. Horrocks, *Inorg. Chem.*, 1966, **5**, 1968; C. A. McAuliffe and D. W. Meek, *Inorg. Chem.*, 1969, **8**, 904; E. Ercolani, J. V. Quagliano and L. N. Vallarino, *Inorg. Chim. Acta*, 1973, **7**, 413.
- L. Sacconi, F. Mani and A. Bencini, in *Comprehensive Co-ordination Chemistry*, eds. G. Wilkinson, R. D. Gillard and J. A. McCleverty, Pergamon, Oxford, 1987, vol. 5, ch. 50, pp. 45–68.
- A. J. Blake, M. A. Halcrow and M. Schröder, *Z. Kristallogr.*, 1993, **205**, 295.
- A. Miedaner, R. C. Haltiwanger and D. L. Dubois, *Inorg. Chem.*, 1991, **30**, 417.
- Y. V. Roberts, Ph.D. Thesis, University of Edinburgh, 1991; A. J. Blake, Y. V. Roberts and M. Schröder, unpublished work.
- See, for example, F. V. Lovecchio, E. S. Gore and D. H. Busch, *J. Am. Chem. Soc.*, 1974, **96**, 3109 and refs. therein.
- G. A. Bowmaker, P. D. W. Boyd, G. K. Campbell, J. M. Hope and R. L. Martin, *Inorg. Chem.*, 1982, **21**, 1152; G. A. Bowmaker, P. D. W. Boyd and G. K. Campbell, *Inorg. Chem.*, 1982, **21**, 2403; G. A. Bowmaker, P. D. W. Boyd, M. Zvagulis, K. J. Cavell and A. F. Masters, *Inorg. Chem.*, 1985, **24**, 401.
- A. H. Maki, N. Edelstein, A. Davison and R. H. Holm, *J. Am. Chem. Soc.*, 1964, **86**, 4580.
- W. E. Geiger, C. S. Allen, T. E. Mines and F. C. Senftleber, *Inorg. Chem.*, 1977, **16**, 2003.
- B. A. Goodman and J. D. Raynor, *Adv. Inorg. Chem. Radiochem.*, 1970, **13**, 135.
- T. I. Hyde and M. Schröder, unpublished work.
- M. C. R. Symons and D. X. West, *J. Chem. Soc., Dalton Trans.*, 1985, 379.
- M. W. Renner, L. R. Furenlid, K. M. Barkigia, A. Forman, H.-K. Sum, D. J. Simpson, K. M. Smith and J. Fajer, *J. Am. Chem. Soc.*, 1991, **113**, 6891; G. K. Lahiri, L. J. Schlüssel and A. M. Stolzenberg, *Inorg. Chem.*, 1992, **31**, 4991.
- N. Jubran, G. Ginzberg, H. Cohen, Y. Kores and D. Meyerstein, *J. Chem. Soc., Chem. Commun.*, 1982, 517; *Inorg. Chem.*, 1985, **24**, 251.

- P. Chmielewski, M. Grzeszczuk, L. Latos-Grazynski and J. Lisowski, *Inorg. Chem.*, 1989, **28**, 3546; L. Latos-Grazynski, M. M. Olmstead and A. L. Balch, *Inorg. Chem.*, 1989, **28**, 4066; L. R. Furenlid, M. W. Renner, D. J. Szalda and E. Fujita, *J. Am. Chem. Soc.*, 1991, **113**, 883; M. P. Suh, H. K. Kim, M. J. Kim and K. Y. Oh, *Inorg. Chem.*, 1992, **31**, 3620.
- 28 L. Sacconi and S. Midollini, *J. Chem. Soc., Dalton Trans.*, 1972, 1213; L. Sacconi, C. A. Ghilardi, C. Mealli and F. Zanobini, *Inorg. Chem.*, 1975, **14**, 1380; L. Sacconi, P. Dapporto and P. Stopponi, *Inorg. Chem.*, 1976, **15**, 325; 1977, **16**, 224; P. Dapporto, G. Fallani and L. Sacconi, *Inorg. Chem.*, 1974, **13**, 2874; A. Gleizes, M. Dartiguenave, Y. Dartiguenave, J. Galy and H. F. Klein, *J. Am. Chem. Soc.*, 1977, **99**, 5187; C. Bianchini, D. Masi, C. Mealli and A. Meli, *Cryst. Struct. Commun.*, 1982, **11**, 1475; F. Cecconi, S. Midollini and A. Orlandini, *J. Chem. Soc., Dalton Trans.*, 1983, 2263.
- 29 L. Porri, M. C. Galazzi and G. Vitulli, *Chem. Commun.*, 1967, 228; C. Mealli, P. Dapporto, V. Sriyunyongwat and T. A. Albright, *Acta Crystallogr., Sect. C*, 1983, **39**, 995; C. O. Dietrich-Buchecker, J.-M. Kern and J.-P. Sauvage, *J. Chem. Soc., Chem. Commun.*, 1985, 760.
- 30 D. C. Bradley, M. B. Hursthouse, R. J. Smallwood and A. J. Welch, *J. Chem. Soc., Chem. Commun.*, 1972, 872.
- 31 A. J. Blake, M. A. Halcrow and M. Schröder, *J. Chem. Soc., Chem. Commun.*, 1991, 253.
- 32 A. J. Blake, R. O. Gould, A. J. Holder, A. J. Lavery and M. Schröder, *Polyhedron*, 1990, **9**, 2919; J. A. Clarkson, R. Yagbasan, P. J. Blower and S. R. Cooper, *J. Chem. Soc., Chem. Commun.*, 1989, 1244; S. K. Kano, R. S. Glass and G. S. Wilson, *J. Am. Chem. Soc.*, 1993, **115**, 592.
- 33 A. J. Blake, R. O. Gould, A. J. Holder, T. I. Hyde, G. Reid and M. Schröder, *J. Chem. Soc., Dalton Trans.*, 1990, 1759.
- 34 H. R. Hays and D. J. Peterson, in *Organic Phosphorus Compounds*, eds. G. M. Kosolapoff and L. Maier, Wiley-Interscience, New York, 1972, vol. 3, ch. 6, pp. 343–346.
- 35 G. M. Sheldrick, SHELLX 76, program for crystal structure determination, University of Cambridge, 1976.
- 36 P. R. Mallinson and K. W. Muir, ORTEP II, interactive version, *J. Appl. Crystallogr.*, 1985, **18**, 51.
- 37 R. O. Gould and P. Taylor, CALC, program for molecular geometry calculations, University of Edinburgh, 1985.
- 38 D. T. Cromer and J. B. Mann, *Acta Crystallogr., Sect. A*, 1968, **24**, 321.

Received 1st February 1993; Paper 3/00596H